INTEGRATED DYNAMIC RADIO RESOURCE MANAGEMENT OF WIRELESS COMMUNICATION SYSTEMS

BY KEVIN GANG CHEN

A thesis submitted to the

Graduate School—New Brunswick

Rutgers, The State University of New Jersey

in partial fulfillment of the requirements

for the degree of

Master of Science

Graduate Program in Electrical Engineering

Written under the direction of

Professor Roy Yates

and approved by

New Brunswick, New Jersey

May, 1996

ABSTRACT OF THE THESIS

Integrated Dynamic Radio Resource Management of Wireless Communication Systems

by Kevin Gang Chen, M.S.

Thesis Director: Professor Roy Yates

The rapid growth in the demand for mobile communications has led the industry into an intense research and development effort directed towards a new generation of cellular systems. One of the important objectives in the development of these systems is increasing the capacity while maintaining the required quality of service. The radio spectrum allocated by regulators is both limited and expensive. Therefore, it is desirable to develop better radio resource allocation schemes that use the spectrum more efficiently than in systems of today. Radio resource management consists of several subtasks, including base station assignment, dynamic channel allocation (DCA), transmitter power control, new call admission control and handoff management. While prior research mostly focused on one or two subtasks, this thesis studies Integrated Dynamic Radio Resource Management (IDRRM) algorithms which combine all the subtasks.

A simulation environment (MADRAS V3) with mobile users has been developed for both one and two dimensional systems. It includes both a Manhattan-like road grid structure for the two dimensional case and a highway structure for the one dimensional case, with corresponding mobility, teletraffic and propagation models. Using this simulation environment, we evaluate a collection of IDRRM algorithms in terms of statistics such as call blocking, call dropping, average handoff distance, average handoffs per call and average transmitted power. We find that interactions among the components of an IDRRM algorithm can be significant and must be considered in the design of a complete system.

Acknowledgements

I would like to thank Professor Roy Yates for his generous support and encouragement throughout the course of this research. I would like to thank Professor David J. Goodman for introducing me to the challenging field of wireless communications and giving me a chance to work at the Wireless Information Network Laboratory (WINLAB). I would like to thank Professor Jack Holtzman and Professor Christopher Rose for carefully reading this thesis and giving several valuable suggestions. I also would like to thank my fellow students and staff at WINLAB for their support and help throughout my stay here.

Dedication

This thesis is dedicated to my Father, Mother and my Wife.

Table of Contents

List of Tables

List of Figures

List of Abbreviations

ACP-DCA Active Channel Preservation Dynamic Channel Allocation. (Chapter 2)

ADCPC Asynchronous Distributed Constrainded Power Control. (Section 1.5)

BER Bit Error Rate.

BS Base Station.

CAI Common Air Interface.

CDMA Code Division Multiple Access.

COMBH Combined RSSI and SIR Based Handoff. (Section 1.7)

DCA Dynamic Channel Allocation. (Section 1.4)

DCPC Distributed Constrainded Power Control scheme. (Section 1.5)

DPC-ALP Distributed Power Control–Active Link Protection scheme. (Section 1.6)

FCA Fixed Channel Allocation. (Section 1.4)

FER Frame Error Rate.

FDMA Frequency Division Multiple Access.

HO Handoff, or Handover.

IAC Interactive Admission Control. (Section 1.6)

IDRRM Integrated Dynamic Radio Resource Management. (Section 1.8)

LI-DCA Least Interference channel Dynamic Channel Allocation. (Section 1.4)

LOS Line-Of-Sight.

MADRAS Mobility And Dynamic Resource Allocation Simulator. (Chapter 4)

MAX-MIN Power control scheme. (Section 1.5)

MPH Minimum Power Handoff algorithm. (Section 1.7)

MS Mobile Station.

N-IAC Non-Interactive Admission Control. (Section 1.6)

N-LOS Non-Line-Of-Sight.

PCS Personal Communication Systems.

QoS Quality of Service.

RSSI Received Signal Strength Indicator .

RSSIBH RSSI Based Handoff. (Section 1.7)

SAS Soft And Safe IAC algorithm. (Section 1.6)

SIR Signal to Interference Ratio.

SIRBH SIR Based Handoff. (Section 1.7)

TDMA Time Division Multiple Access.

Chapter 1
Radio Resource Management

1.1 Introduction

The rapid growth in the demand for mobile communications has led the industry into an intense research and development effort directed towards a new generation of cellular systems. One of the important objectives in the development of these systems is increasing the capacity while maintaining the required quality of service. The system capacity, as measured by the number of users a network can support, is fundamentally dependent on the common air interface (CAI) over which users communicate. In particular, the system capacity depends on the amount of spectrum the regulators allocate, the size of the radio coverage area from a base station (BS), and the amount of interference a particular radio link can tolerate. The spectrum allocated by the regulators is not only very limited, but also very expensive as seen in the recent PCS license auction. Therefore, it is desirable to develop better radio resource allocation schemes that use the radio spectrum more efficiently than the resource allocation algorithms in systems of today.

In cellular communication systems, the maintenance of calls between BSs and mobile stations (MS) requires the establishment of radio connections. For each call, the connection consists of four elements

- The assigned BS with which the MS is communicating,
- The allocated channel (carrier frequency or time slot),

- The downlink (BS) transmitted power,
- The uplink (MS) transmitted power.

Due to the changing load and interference caused by mobility, these elements should be adapted dynamically during the call to minimize the global interference level and the number of handoff events. This is the task of radio resource management.

While prior research mostly focused on adaptation of one or two elements of the four, this research combines the adaptation of all four elements. A simulation environment (MADRAS V3) has been developed for both one and two dimensional systems. It includes both a Manhattan-like road grid structure (two dimensional case) and a highway structure (one dimensional case), with corresponding traffic and propagation models. Using this simulation environment, a collection of integrated dynamic resource management algorithms are evaluated in a system with mobile users.

1.2 Subtasks of Radio Resource Management

The objective of a radio resource management scheme is to assign a base station, a channel and a pair of transmitter powers to as many communication links as possible at any moment of time, subject to the constraint that the quality of all links should be above a certain threshold. The radio resource management algorithm consists of several subtasks, namely,

- *Base Station Assignment* — The assignment of an appropriate BS to which the MS can communicate.
- *Channel Allocation* — The allocation of a channel which provides sufficient link quality to the call.

- *Transmitter Power Control* — The process of constantly adjusting the transmitter power of the MS and/or the BS to reduce the overall system interference level.

- *New Call Admission Control* — The admission check when an MS initiates a new call request.

- *Handoff* or *Handover (HO)* — The switching procedure used by an MS to change its communication from one BS to an adjacent one when the MS is moving out of the coverage area of the prior BS.

The radio resource management for an MS starts when the MS is trying to make a phone call and ends when the call is finished or dropped. The radio

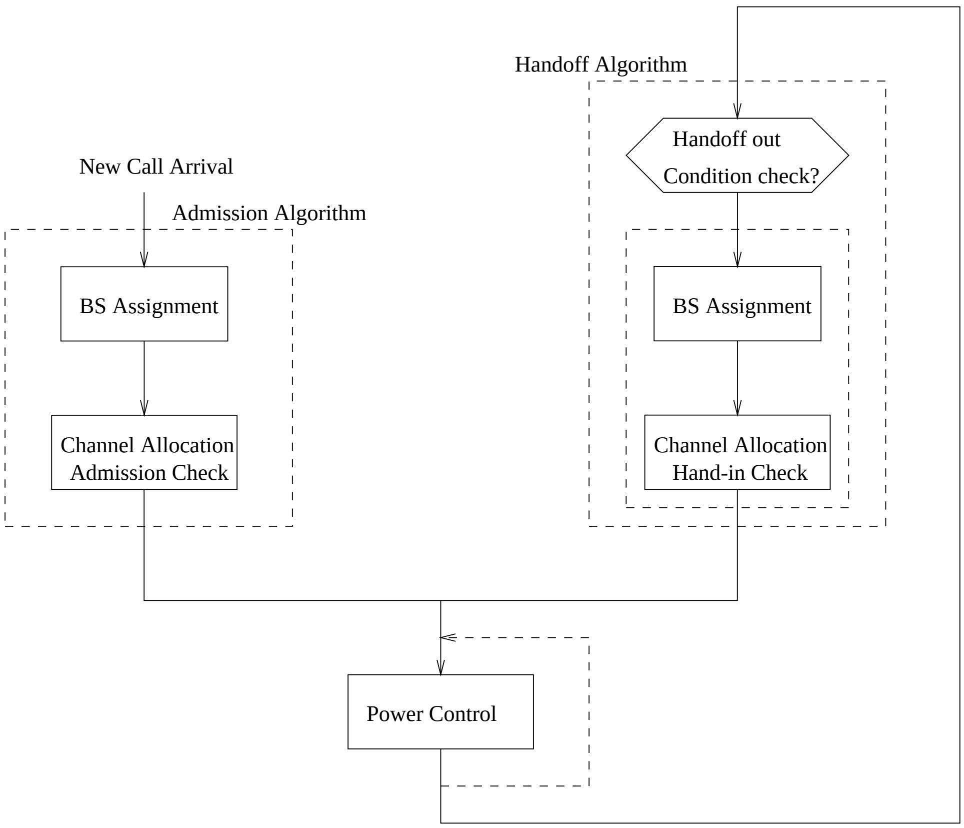

Figure 1.1: Flowchart and Subtasks of Radio Resource Management

resource management process is shown in Figure 1.1. When a new call arrives, a new call admission procedure is invoked. The new call is assigned a BS and allocated a channel (frequency/timeslot or code) subject to an admission check. If it is successfully allocated a channel and passes the admission check, the conversation begins and the transmitter power is adjusted constantly by the power control scheme. During the call, the link quality is checked constantly and if certain handoff criteria are met, as specified by the handoff algorithm, a handoff attempt is initiated for this MS. The handoff algorithm will assign a new BS (in handoff algorithms that permits intra-cell handoffs, the new BS might be the same as the old BS), allocate a new channel. A hand-in condition check is then performed to see if quality of the new link is sufficient. If so, the MS will use the new BS-channel pair to communicate with the fixed network. Otherwise, the MS will keep using the old BS and channel and will try to handoff again later until it succeeds or until it is dropped because the link quality is too poor.

1.3 Base Station Assignment

Each BS communicates with a number of mobiles residing within its radio coverage area. When a newly arrived MS sends out a service request, it must be assigned to a nearby BS because each BS has a limited radio coverage area. This area, which is referred to as a cell, is defined by the received signal strength. Base station reassignment is also needed when an MS is moving out of its original cell and needs to be handed off into a new cell. One natural thought is to assign the mobile to the geographically nearest BS. However, in a real system, it is very hard to measure the exact distance from the MS to different BSs and this distance information is generally not available in current systems. Besides, in a practical situation with shadow fading and interference, the nearest BS does not necessarily provide the best communication link to the MS.

A better way is to assign the BS to which the MS has the least path loss. We assume each base station continuously transmits a beacon signal (pilot tone) at a constant power level. The new MS (or in case of handoff, the handoff MS) listens and compares the strength of the received pilot tone signal. The MS i is assigned to the BS with the strongest received pilot tone signal:

$$\text{BS of MS i} = \arg\max_{j \in B} P_c G_{ij}$$

where P_c is the transmit power of pilot signal which is same for all the BSs, G_{ij} is the gain factor due to path loss and fading between the MS i and BS j, and B is the set of BSs in the system.

1.4 Channel Allocation

The available frequency spectrum is an important resource of the wireless system. The efficient use of it is necessary to achieve a high system capacity. Present-day systems use fixed channel allocation (FCA), which divides the total available channels into several groups. Each cell can only use one group of channels. The same group of channels can only be reused in cells some distance away. This reuse distance is determined by the minimum acceptable signal to cochannel interference ratio (SIR) of the system. The farther the reuse distance is, the lower the cochannel interference and the higher SIR the radio link can achieve. The cochannel interference is kept to acceptable limits by the reuse distance between the cells. The number of channel groups, which is also called reuse factor, is determined by the reuse distance.

In contrast to FCA, with dynamic channel allocation (DCA), there is no fixed relationship between the cells and the channels that they use. Each cell may allocate any channel to the MS as long as that channel provides sufficient radio link quality. The DCA algorithm could be used on a call-by-call basis to achieve time-varying frequency reuse patterns that dynamically attempt to minimize mutual interference among all active calls. DCA has the potential to efficiently reuse limited radio spectrum by statistically multiplexing radio channels provided by a cluster of BSs. Without the need for frequency planning, TDMA or FDMA systems with DCA can serve dynamic and nonuniform traffic demands and achieve a higher capacity than FCA. [11, 37, 35, 15]

DCA can be done by adapting to either the traffic loading at the base station or the interference on the channels or both. In a traffic adaptive system, each cell site examines channel usage in neighboring cells and others that might interfere, and avoids those channels when assigning a channel to a new MS. A particularly simple system is channel borrowing, in which a fixed channel assignment is generally followed, but when a cell is overloaded it can use idle channels belonging to a neighbor's fixed allocation. In traffic adaptive DCA schemes, communication of channel usage information among cells or to a central controller is required.

In contrast, the interference-adaptive DCA algorithm can be distributed. The BS (and MS) controls the channel allocation of a call based on its local information without the need to communicate with other BSs or with a central controller. At the time of a new call or a handoff request the interference level is measured in all the free channels. A channel is then assigned if it satisfies certain interference or SIR requirements. In this case, there may be different choices among acceptable channels. Selecting the least-interfered channel is considered to be a robust algorithm [28]. As an alternative, selection of a channel such as the worst but still acceptable channel may lead to greater capacity but may also lead to possible instability [28]. In a system with static mobiles, a number of distributed measurement-based DCA schemes were compared in [7] and the Least Interference Algorithm had the best overall performance. The Least Interference channel DCA scheme (LI-DCA) [33, 2, 38, 27, 1, 10] described next, is used as a reference scheme in this study.

Least Interference channel DCA scheme (LI-DCA): When a new MS is assigned to a BS i, or a ongoing call is trying to handoff to BS i, BS i measures the interference $I_i^{(k)}$ on each channel k that has not been assigned to another MS. The MS is then assigned to a channel with the least interfering power, that is, the channel h such that

$$h = \arg\min_{k \in C_i} \{I_i^{(k)}\}$$

where C_i is the set of channels at BS i that are not occupied by the other MSs.

This interference-adaptive DCA scheme has the advantage that the MS and its BS can control the channel assignment of a call without the need to communicate with other BSs or with a central controller. This distributed algorithm is incorporated in the cordless telecommunication systems CT-2, CT2 Plus, and DECT-Pan European Cordless Phone [33, 38, 11, 1].

Channel allocation is closely related to call admission and handoff because channel allocation normally occurs at the time of a new call or a handoff request and whether a channel is successfully allocated or not determines the success of call admission or handoff attempt. If no channel is found the call is blocked, queued, or even dropped. An Active Channel Preservation DCA (ACP-DCA) scheme which is both traffic and interference adaptive is proposed in Chapter 2. It combines the channel allocation and call admission in an attempt to prevent new admitted calls from causing active calls to be dropped.

1.5 Transmitter Power Control

Transmitter power control decreases the interference that one mobile causes to other mobiles and thereby not only dramatically improves the quality of calls but also increases the system capacity. Initial work on power control centered on schemes that try to maintain a constant received power levels at both the BS and the MS [40, 13, 34]. Later studies [36, 48, 17] indicated that for a given link quality requirement the system capacity can be maximized by adjusting the transmitter power such that all admitted connections operate at the same SIR. This SIR-balancing power control scheme is also referred to as MAX-MIN scheme, because it maximizes the minimum SIR over all the radio links. Distributed power control schemes, iteratively adjusting the power of the individual links based only on measurements in that link, can be used to implement these SIR-balancing schemes, and have been shown to achieve similar performance [47, 16, 12, 32].

Other than the MAX-MIN SIR power control scheme, a simpler algorithm is for each mobile to just increase its transmit power when the SIR is inadequate and decrease its transmit power when the SIR is more than adequate. Each MS can also be trying to achieving an individual target SIR corresponding to distinct quality of service (QoS). Zander and Grandhi have also investigated a distributed constrained power control scheme where there is a limit on the maximum output power due to the battery capacity limitations [49, 19, 20]. Recent studies have looked at power control schemes based on bit error rate (BER) or frame error rate (FER), which are physically measurable at the BS and the MS and are also monotone functions of the SIR [29]. Yates and Huang [46, 45] and Hanly [25] proposed a more sophisticated Minimum Power Algorithm which combined the base station assignment and power control. Yates has also proposed a general framework for uplink power control schemes [44].

This thesis considers an asynchronous distributed constrained SIR-balancing power control scheme (ADCPC) as proposed in [20]. Each active mobile adjusts its transmit power to achieve a common target SIR (γ_t) every T_{pc} seconds. So does the BS on downlink transmit power. In actual implementation, each BS and MS pair frequently measures the uplink and downlink SIRs and exchange this information through an associated control channel.

The transmit powers are adjusted asynchronously at each of the M mobile stations based on the following:

$$P_i' = \min\{P_{\max}, \gamma_t \frac{P_i}{\gamma_i}\}, 1 \leq i \leq M \tag{1.1}$$

where P_i is the mobile transmit power before the adjustment, and P_i' is the power after the adjustment, γ_t is the common target SIR each mobile is trying to achieve, and γ_i is the uplink SIR measured by the BS. The maximum transmit power, $P_{\max}$, is determined by the practical hardware constraints imposed on the mobile. The situation on the downlink is the similar, but the maximum transmit power for the downlink may be much higher than that of uplink.

It is shown that in a system with stationary MSs, for every target SIR, the DCPC and ADCPC schemes converge to a stationary positive power vector under which some receivers exactly achieve their target SIR with transmitter power strictly less than the maximum allowable power, and the rest are below their target SIR with transmitter power equal to maximum power[20]. However, when the MSs are moving very fast, the gain matrix will also be changing very fast due to the change in shadow fading condition. The behavior of this ADCPC scheme will be different. The effect of fast moving mobile users on the ADCPC scheme is investigated in this thesis by simulation methods and the results are given in Chapter 5.

1.6 Admission Control

A new arriving MS requires a new communication link, i.e., a BS and a channel. To guarantee a certain degree of link quality for the active calls, as well as low outage and blocking probabilities, certain admission control must be carefully exercised. Call admission control is closely related to the channel allocation scheme. Different channel allocation schemes imply different admission control algorithms. For example, with FCA, a simple admission control algorithm is to admit any new call if there are any available free channels. But with the LI-DCA scheme mentioned above, a free channel (which means it is not used at this BS) might already be used by one or more neighboring BSs, and hence will have unacceptably high interference to be used in this BS. Different admission control schemes are needed for DCA.

A centralized admission control algorithm is studied in [6]. This algorithm requires the knowledge of the link gains matrix. In [3], admission control schemes are divided into two general categories. One is the Non-Interactive Admission Control (N-IAC), where admission decisions are instantaneously made based on the system state. The other is an Interactive Admission Control (IAC), under which the new mobile is permitted to interact with one or more potential channels before a decision is made. A Soft and Safe (SAS) interactive admission control algorithm, which accepts a new MS if and only if the active mobiles and the new one can be supported at their target SIRs, is studied there and compared with two N-IAC schemes. The SAS algorithm is shown to perform better than the N-IAC schemes but converges slowly. The SAS algorithm is type I and II error free in static MS situation, where type I error occurs when a new MS is erroneously accepted and results in an outage, and type II error occurs when a new MS is erroneously rejected while could be supported along with the other active MSs. A Fast SAS algorithm which converges faster with a little performance penalty is also proposed. Another IAC scheme, the Distributed Power Control with Active Link Protection (DPC-ALP) algorithm, which is similar to the SAS algorithm, has been studied [5]. Both SAS and DPC-ALP schemes protect the active links by gradually powering up the new link.

The IAC algorithms may suffer from slow convergence. Also in IAC schemes, the new MS can only interact with one channel at a time, and needs some time to find if the attempt has failed before it can try again on a different channel. So with IAC, the admission procedure may be very long, although the Fast SAS algorithm may shorten this time. The SAS algorithm is type I and II error free when the MSs are stationary, but in a real system with shadow fading variation and moving MSs, the gain factors between the BSs and the MSs will change with time. Hence outages may still occur despite the use of the SAS algorithm.

As our reference system, we consider distributed dynamic radio resource allocation schemes that integrates both LI-DCA and SIR-balancing ADCPC, with the following N-IAC policy.

Admission SIR Threshold policy: After a MS is assigned to a base station, the BS will look for a channel with the least interference. The power required to achieve the SIR threshold, γ_{new}, is estimated and compared to the maximum allowable power, $P_{\max}$. If the estimated power is less than $P_{\max}$, the new call is admitted. Otherwise, the request to set up a new call is denied, and we say that the new call is blocked.

Later in next chapter, we present a new Active Channel Preservation DCA and admission control algorithm.

1.7 Handoff Algorithms

The demand for high capacity in the future wireless communication network will lead to very small cells (microcells). Consequently an MS will travel over more cells during a call than in the systems of today. In order to maintain reliable communications in a microcellular system, new and better handoff algorithms must be developed. The handoff algorithms should be able to maintain an adequate link quality during and after the handoff. A fast handoff is desirable so that a subscriber hardly realizes the service interruption. However, a balance should be kept between minimizing the delay in handoff and minimizing the number of unnecessary handoffs.

Many handoff algorithms have been studied. Most of them focus on handoff algorithms based on received signal strength index (RSSI). In [41, 42, 50] the

RSSI based handoff process itself is studied, and the effect different parameter values are compared in order to reduce the Ping-Pong effect, which happens when a MS is handed off back and forth between two or more BSs. In [26, 31, 23, 14] the RSSI based handoff scheme is studied in the context of system performance and capacity.

An SIR Based Handoff algorithm was proposed in [9] for a power controlled multichannel system. In this system, each user aims for a target SIR, γ_{t}, and handoffs are made when the absolute SIR drops below a certain threshold, γ_{ho}, which is normally less than γ_{t}. As pointed out in [9], SIRBH causes cell dragging and inhibits handoffs near geographical cell boundaries. A Minimum Power Handoff (MPH) Algorithm was proposed in [8] which combines the power control and handoff tasks and minimizes the transmitter power of the system.

A handoff is a complex procedure which can be roughly divided into four steps. The first step, a handoff attempt is initiated when certain trigger condition is satisfied. This condition determines when a handoff attempt will be initiated to hand a call out of the current cell, so it is referred to as the Hand-out Policy. The second step, the decision algorithm finds a new BS that is suitable for the call to handoff. The third step, a channel allocation and associated handoff admission policy, (referred to as the Hand-in Policy) is employed to decide whether the call can be handed into this BS and allocate a channel to the handoff call. Some handoff algorithms combined steps 2 and 3 by assigning the BS and the channel together [8]. Finally both the network and the mobile must switch quickly before the link quality of the call deteriorates. When current channel cannot provide sufficient radio link quality due to high interference and the MS is still far away from any other BS, an intra-cell handoff, or channel reallocation, is needed. In this case, the MS is reallocated another channel which will provide better link quality for the MS at the same BS. The same four steps as above could be employed to the intra-cell handoff except that in step 2 the MS stays at the old BS.

In Step 1, the Hand-out policy typically uses measurements of the received signal strength indication(RSSI) and/or SIR and/or BER to decide when and where to handoff. There are thresholds for received signal strength and SIR, and hysteresis and system timers may be used to preclude a mobile making repeated handoffs.

As for the Hand-out policy of the handoff algorithms, we have studied the following three policies

SIR based (SIRBH): If the SIR of a terminal falls under certain threshold ($\gamma_{\mathrm{h-out}}$), then the terminal tries to make a handoff to the BS with the strongest received pilot tone. This may be an intra-cell handoff if the original BS is the BS with the strongest received pilot tone. In either case, a successful handoff happens only if the terminal can find a channel using the dynamic channel allocation scheme.

Received Signal Strength based (RSSIBH): If the RSSI of another BS's pilot tone is T_{hy}(dB) higher than that of the original BS's, then the MS tries to make an inter-cell handoff to that BS. A successful handoff happens only if the MS can find a channel under DCA. No intra-cell handoff is made in this scheme.

Combined SIR and RSSI based (COMBH): If either the SIR or the RSSI condition is satisfied, then the mobile tries to make inter- or intra-cell handoff. A successful handoff happens only if the DCA algorithm can find an acceptable channel for the mobile.

1.7.1 Prioritized Handoff

Step 3 of the handoff algorithm mentioned above, the channel allocation scheme and the associated admission policy (Hand-in Policy) is part of the general channel allocation algorithm. In some channel allocation strategies, the handoff requests are handled exactly the same manner as the new calls. Obviously, such schemes suggest that the probability of forced termination of an ongoing call due to unsuccessful handoff is similar to or even much higher than the probability of blocking an originating call because handoff calls are normally close to the cell boundary, hence they generally face more interference and have higher path loss than ordinary new calls. From a subscriber's point of view, however, a forced termination of an ongoing call is much more annoying than a blocking of a new call attempt. When the system is more heavily packed, it becomes more difficult to find a channel for a handoff call. Hence a number of prioritized handoff schemes have been proposed which aim to minimize both the probability of forced termination of calls in progress due to handoff failures, and the degradation in spectrum utilization [26, 14, 43]. These prioritized handoff schemes generally employ different channel allocation schemes or admission policies for handoff calls from new calls to decrease the probability of forced termination at the expense of a tolerable increase in call blocking probability and hence, a decrease in total carried traffic.

The Guard Channel Concept

The "guard channel" concept was introduced in the mid-1980s [26]. It offers a general means of improving the probability of successful handoff by simply reserving a number of channels exclusively for handoffs. The remaining channels can be shared equally between handoffs and originating calls.

The penalty is the reduction of total carried traffic due to the fact that fewer channels are granted to originating calls. This disadvantage can be bypassed by allowing the queuing of originating calls. Intuitively, we can say that this is feasible because originating calls are considerably less sensitive to delay than handoff requests.

Another shortcoming of the employment of guard channels, especially with

FCA, is the risk of inefficient spectrum utilization. Careful planning need to be made to decide the optimum number of channels reserved for handoff calls.

Different Thresholds for handoff calls and new calls

In DCA schemes, different admission SIR and/or RSSI thresholds can be employed on handoff calls and new calls to give priority to handoff calls. For example, with LI-DCA scheme, an SIR threshold $\gamma_{\mathrm{h-in}}$ can be used for hand-in admission instead of γ_{new} for new call admission. The relationship between these different SIR thresholds is explained below.

γ_{floor} is the minimum SIR requirement for the radio link. If the SIR of a radio link is below γ_{floor}, the quality is not acceptable and after a certain time specified by a system timer, the call will be dropped. γ_{t}, which is higher than γ_{floor}, is the target SIR each MS and BS will try to achieve by adjusting their transmitter power. A margin should be kept between γ_{t} and γ_{floor} because of the shadow fading condition, the movement of the mobiles and the need for convergence time of the power control algorithm. The admission SIR threshold, γ_{new}, is normally higher than or equal to the target SIR, γ_{t}. In the LI-DCA scheme, $\gamma_{\mathrm{h-in}}$ could range from γ_{floor}, corresponding to full priority for handoff calls, to γ_{new} for no priority. If SIRBH is used, the hand-out SIR threshold, $\gamma_{\mathrm{h-out}}$, will range between γ_{floor} and γ_{t}, but will also be less than $\gamma_{\mathrm{h-in}}$ to give some SIR hysteresis for handoff calls. So we have

$$\gamma_{\mathrm{floor}} < \gamma_{\mathrm{t}} \leq \gamma_{\mathrm{new}}$$

$$\gamma_{\mathrm{floor}} \leq \gamma_{\mathrm{h-in}} \leq \gamma_{\mathrm{new}}$$

$$\gamma_{\mathrm{floor}} \leq \gamma_{\mathrm{h-out}} \leq \gamma_{\mathrm{t}}$$

$$\gamma_{\mathrm{h-out}} < \gamma_{\mathrm{h-in}}$$

1.8 Integrated Dynamic Radio Resource Management

While much of the prior work on radio resource management primarily focuses on one subtask only, some recent work addresses the joint optimization of two or more subtasks, such as power control and base station assignment [46, 45, 25]. [18] has shown that DCA and power control can greatly increase the system capacity. Recent work began to study an Integrated Dynamic Radio Resource Management (IDRRM) algorithm which combines all the subtasks together in an one-dimensional highway cellular system [9, 8, 4]. We will extend this work by studying integrated dynamic radio resource management algorithms in both one and two dimensional, macrocellular and microcellular systems.

Chapter 2

Dynamic Channel Allocation with Active Channel Preservation

It has been shown that both DCA and transmitter power control can greatly enhance system performance and increase system capacity [11, 37, 35, 16, 18]. We consider narrowband cellular systems with distributed dynamic resource management schemes that integrate both DCA and asynchronous distributed SIR-balancing power control. When a new call is set up, a channel is assigned and the transmitter power is chosen to yield the required SIR. The transmission of the new mobile will increase the interference faced by other MSs on that channel, requiring re-adjustment of the transmitter powers of those MSs. Occasionally, this might cause the SIR of some active links to fall below the minimum required SIR, causing those calls to be handed off to other channels (intra-cell handoff) or terminated (dropping). In principle, central control with complete information on all bases-to-mobiles connectivity could foresee such an event and block the admission of the new user. However, such a central control is not a practical solution. Two similar IAC distributed power control schemes, which protect the active links by gradually powering up the new link, have been proposed [4, 5]. As we have mentioned, the process of these IAC schemes is slow, since the user can try only one channel at a time, and needs some time to find if an attempt has failed before trying again on a different channel.

We present an alternative non-interactive approach — Active Channel Preservation DCA and admission control scheme (ACP-DCA). This scheme represents an extension of an admission control scheme proposed by Timor [39] to systems with transmitter power control. Whenever a new MS arrives, the assigned BS of the MS (i.e., the BS with the strongest pilot tone signal) attempts to predict what the quality of the other links will be after the new MS has been admitted. The prediction will be based on the information from the neighboring BSs about their channel usage, link quality (SIR) and RSSI, and the information from the new MS about the measured RSSI of all the neighboring BS pilot tones. Ideally, the new MS will be admitted only if there exists at least one channel such that the new link will have a required SIR, while all active links will stay above a threshold SIR. In this case, the new call is assigned one of these channels. Otherwise, the new call is blocked.

To perform this prediction the BS needs some data from adjacent BSs. This data can be measured at each BS and periodically transfered to the neighboring BSs. Only the information from neighboring BSs are needed because only those BSs might be adversely affected by the new link. After the new MS is admitted, it will join all the other active MSs and its radio resources will be managed by the regular radio resource management scheme.

Mobility can cause active links to drop below the required SIR, requiring handoff to other BSs and/or other channels. The periodically exchanged information by the BSs can also assist the active MSs to perform handoff, by predicting the conditions after the handoff, in order to check that no other active link will be dropped as a result of the handoff.

2.1 Active Channel Preservation

With Dynamic Channel Allocation, all bases have access to all channels $k \in C$, where C is the set of all the channels in the system. We assume that interference from other channels is negligible and consider only cochannel interference. The system performs the asynchronous distributed constrained power control of

Equation (1.1) which tries to achieve a common SIR for all users, subject to a maximum power constraint, $P_{\max}$. We only consider the uplink here due to an implementation reason which we will explain later.

In a narrowband system like TDMA/FDMA, at most one MS can be using the same channel (frequency band or time slot) to communication with the same BS at one time. Suppose M_k is the set of mobiles that uses channel $k \in C$ in the system. On each channel k, we index the BS-MS pair by i. The uplink SIR on channel k at BS i, γ_i, is

$$\gamma_i^{(k)} = \frac{G_{ii}P_i^{(k)}}{I_i^{(k)}} = \frac{G_{ii}P_i^{(k)}}{\sum_{j\in M_k}^{j\neq i} G_{ji}P_j^{(k)} + n_i^{(k)}} \tag{2.1}$$

where $P_i^{(k)}$ is the power transmitted by MS $i \in M_k$, G_{ji} is the path loss coefficient from MS $j \in M_k$ to BS i , G_{ii} is the path loss coefficient from MS $i \in M_k$ to its own BS i , $I_i^{(k)}$ is the total uplink interference (plus noise $n_i^{(k)}$) at BS i.

If a new mobile m, which is assigned to BS m, begins to transmit in channel k with an uplink power $P_m^{(k)}$, the SIR of the new link will be

$$\gamma_m^{(k)} = \frac{G_{mm}P_m^{(k)}}{I_m^{(k)}} \tag{2.2}$$

The above equation can also be written as

$$P_m^{(k)} = \gamma_m^{(k)}\frac{I_m^{(k)}}{G_{mm}} \tag{2.3}$$

This new MS will add interference to all active links, resulting in a new SIR γ_i^* of MS $i \in M_k$,

$$\gamma_i^{*(k)} = \frac{G_{ii}P_i^{(k)}}{I_i^{(k)} + \Delta I_i^{(k)}} = \frac{\gamma_i^{(k)}}{1 + \frac{\Delta I_i^{(k)}}{I_i^{(k)}}} \tag{2.4}$$

where

$$\Delta I_i^{(k)} = G_{mi}P_m^{(k)} = \gamma_m^{(k)}\frac{G_{mi}I_m^{(k)}}{G_{mm}} \tag{2.5}$$

is the increase of the uplink interference of MS-BS pair i caused by the new MS m.

Thus, the SIR of each active link i is reduced by the factor of

$$1 + \frac{\Delta I_i^{(k)}}{I_i^{(k)}} = 1 + \frac{G_{mi} P_m^{(k)}}{I_i^{(k)}} = 1 + \gamma_m^{(k)} \frac{I_m^{(k)} G_{mi}}{I_i^{(k)} G_{mm}} \tag{2.6}$$

Because each MS is performing the distributed constrained power control mentioned in section 2.3, now MS i will try to adjust its power to achieve the target SIR γ_{t}. After MS i has done one iteration of power adjustment, from Equation (1.1), the new transmit power of MS i will be

$$P_i^{'(k)} = \min\{P_{\max}, \gamma_{\mathrm{t}} \frac{P_i^{(k)}}{\gamma_i^{*(k)}}\} = \min\{P_{\max}, \gamma_{\mathrm{t}} \frac{I_i^{(k)} + \Delta I_i^{(k)}}{G_{ii}}\} \tag{2.7}$$

The new SIR after the power adjustment will be

$$\gamma_i^{'(k)} = \min\{\frac{P_{\max} G_{ii}}{I_i^{(k)} + \Delta I_i^{(k)}}, \gamma_{\mathrm{t}}\} \tag{2.8}$$

It might be less than γ_{t}, or even less than γ_{floor} , which means that this channel k is so densely packed, that the quality of the active link will deteriorate if the new MS is admitted into this channel.

Let C_m be the set of channels which are free at BS m. Let γ_{new} be the admission SIR for new MSs. It is a control parameter of the system which can be fixed, or adaptive to the traffic load, or to the type of data. (In the case of a handoff, this should be replaced by a different parameter γ_{h-in}, which may give priority to handoff calls.) To achieve this SIR on the channel $k \in C_m$, the new MS m has to transmit with power P_m given by

$$P_m^{(k)} = \gamma_{\mathrm{new}} \frac{I_m^{(k)}}{G_{mm}} \tag{2.9}$$

If γ_{floor} is the minimum allowable SIR threshold for the active links, then we require the SIR of all active links after one power control iteration, $\gamma_i^{'(k)}$, to satisfy

$$\gamma_i^{'(k)} \geq \gamma_{\mathrm{floor}} \tag{2.10}$$

for all active links $i \in M_k$, or

$$\min\{\frac{P_{\max} G_{ii}}{I_i^{(k)} + \Delta I_i^{(k)}}, \gamma_{\mathrm{t}}\} \geq \gamma_{\mathrm{floor}} \tag{2.11}$$

for the new call to be set up on channel k. Because $\gamma_{\mathrm{t}} > \gamma_{\mathrm{floor}}$, Equation (2.11) becomes

$$\frac{P_{\max}G_{ii}}{I_i^{(k)} + \Delta I_i^{(k)}} = \frac{P_{\max}G_{ii}}{I_i^{(k)} + \gamma_{\mathrm{new}}\frac{G_{mi}I_m^{(k)}}{G_{mm}}} \geq \gamma_{\mathrm{floor}} \tag{2.12}$$

Equation (2.12), which is the requirement for MS m to be admitted into channel k, can also be written as

$$I_i^{(k)} + \Delta I_i^{(k)} \leq \frac{P_{\max}G_{ii}}{\gamma_{\mathrm{floor}}} \tag{2.13}$$

Equation (2.13) means that the total interference at the uplink of any active link after admitting the new MS m should still be less than $\frac{P_{\max}G_{ii}}{\gamma_{\mathrm{floor}}}$, which is the maximum tolerable interference level of the active link i by using the maximum transmitting power. If for all the active links $i \in M_k$, the above condition is satisfied, then the channel k is deemed acceptable for the new MS m to use. If there is at least one such acceptable channel, then the new MS m is admitted. Otherwise, the new MS m is blocked.

Here we only considered one iteration of power adjustment by the active links. Actually, after the first iterations of all the MSs, the overall interference level sensed by all the MSs, including the new MS m, will become even higher, causing all the MSs to raise their power again. This procedure finally may still lead to possibly early termination of some active calls.

This is why we need the system parameter γ_{new} which is higher than γ_{t} to leave some margin for the active links. When mobile m satisfying Equation (2.12) is admitted into channel k, it's initial power is set to only enough to reach γ_{t}. So the one step increase of the interference caused by this MS is less than in the above derivation. The consequent power adjustments will also be less than those in the above derivation. Although it is possible that eventually the power increases may still lead to early termination of some active calls, but by choosing γ_{new} carefully, we can reduce this early termination to an acceptable level.

2.2 Channel Allocation

Each channel which satisfies the above condition (Equation (2.12)) can be allocated to the new MS m, without causing any active call to be dropped. Within this set of acceptable channels, one specific channel can be chosen according to an allocation strategy.

In Equation (2.12), the left side is actually the maximum SIR achievable after one power adjustment. Pick the channel which maximizes the minimum of such new achievable uplink SIR of active users in this channel after one iteration of power adjustment will leave the greatest margin for the protection of active links.

In particular, each free channel k at BS m can potentially be used by several MSs in neighboring cells. Assume among them, the minimum achievable uplink SIR with the maximum power is

$$\gamma_{\min(k)} = \min_{i \in B(k)} \frac{P_{\max} G_{ii}}{I_i^{(k)} + \Delta I_i^{(k)}} \tag{2.14}$$

where $B(k)$ is the set of BS-MS pairs which is using channel k. Then the channel h that maximizes this minimum achievable SIR $\gamma_{\min(k)}$ over all local free channels k is assigned to the MS, that is

$$h = \arg\max_{k \in C_m} \gamma_{\min(k)} = \arg\max_{k \in C_m} \min_{i \in B(k)} \frac{P_{\max} G_{ii}}{I_i^{(k)} + \Delta I_i^{(k)}} \tag{2.15}$$

and the MS is admitted if and only if

$$\max_{k \in C_m} \gamma_{\min(k)} = \max_{k \in C_m} \min_{i \in B(k)} \frac{P_{\max} G_{ii}}{I_i^{(k)} + \Delta I_i^{(k)}} \geq \gamma_{\text{floor}} \tag{2.16}$$

2.3 Implementation

From Equation (2.12), the implementation of ACP-DCA algorithm requires that, a new MS m or its BS has the knowledge of

- The uplink interference $I_i^{(k)}$ of all (practically, only those within neighboring cells) the active links $i \in M_k$ for all $k \in C_m$, where C_m is the free channels at base station m,

- The gain factors from all the MSs i to their own BSs i, G_{ii},
- The uplink interference $I_m^{(k)}$ on all channels $k \in C_m$ at the BS m,
- The gain G_{mi} from the MS m to different BSs G_{mi},

In one possible implementation, each BS continuously measures the RSSIs and the SIRs on all the channels. Because the power adjustment of the MS is under the control of the BS, the BS also has the knowledge of the transmitter powers of all its active MSs. From this information, the BS can estimate the uplink interferences and path gain coefficients of all its active links and can pass this information to all neighboring BSs. At the setup phase of a new call or when a MS is trying to handoff, it measures the received signal strength of all the nearby BSs' pilot tone signals, and transmits this information to its base station. Based on all the information received, the BS can decide whether to admit the new call and assign the channel. Hence in this ACP-DCA scheme, communication of channel usage information among cells is required.

Figure 2.1 is the pseudo-code of the ACP-DCA scheme.

```
PROCEDURE ACPDCA(MS i; BS m; SIR GAMMAnew)
BEGIN
    AllocChl:= 0;
    MaxMinSIR:= 0;

    FOR each free channel k at BS m
    DO BEGIN
        Intf:= total interference on channel k at BS m;
        PwrRqrd:= GAMMAnew * Intf /GAIN(i,m);
        IF PwrRqrd>Pmax GOTO nextchannel;

        MinNbrSIR:= HUGE_NUM;
        FOR each neighboring BS n using channel k
        DO BEGIN
            j:= MS at BS n using channel k;
            NewNbrSIR:= Pmax * GAIN(j,n)/
                (total interference at n in k + PwrRqrd*GAIN(i,n));
            MinNbrSIR:= min(MinNbrSIR, NewNbrSIR);
        END

        IF MaxMinNbrSIR < MinNbrSIR
        THEN BEGIN
            MaxMinNbrSIR:= MinNbrSIR;
            AllocChl:= k;
        END
nextchannel:
    END

    IF AllocChl==0 THEN fail
    ELSE IF MaxMinNbrSIR<GAMMAfloor THEN fail
    ELSE return AllocChl;
END
```

Figure 2.1: Pseudo-code for ACP-DCA algorithm

Chapter 3
Simulation Scenario

We consider three different cellular structures, namely one dimensional macro-cell, two dimensional macrocell and two dimensional micro-cell. The cells cover a terrain with buildings and geographical characteristics that are known and fixed.

3.1 One Dimensional Macrocell

The one dimensional model represents the macrocellular system along the highway.

Cell Layout

We assume 20 base stations are distributed uniformly along a straight line. All cells are 2 km in length with omni directional base station located at the center of each cell. The straight line is looped at the ends to avoid edge effects so that no matter where a mobile stands, it sees 10 base stations on either side of itself.

Mobility model

Free flowing highway traffic is assumed, which means each vehicle moves along the highway as if there is no other vehicle on the highway. It is assumed the speed and the direction of a mobile are chosen at the beginning of a call and remain constant during the call. Both directions along the highway are equally probable. The speed distribution of the mobiles is modeled as a truncated Gaussian distribution with mean value of 90km/hr and standard deviation of 15km/hr, truncated at a minimum speed of 60km/hr and a maximum speed of 120km/hr ($\pm 2\sigma$ points).

Propagation Model

The signal strength at the receiver depends not only on the distance from the transmitter, but also on various details of the physical environment around the transmitter and receiver, such as terrain, buildings, and other obstacles in the signal path. When the mobile is moving, these environmental factors also change with time and space. The received signal strength is calculated as the emitted power less path loss between the base station and the mobile. We use path loss (L) to denote the local average received signal power relative to the transmit power. This is possible since received power is usually measured as a local spatial average rather than an instantaneous value. In realistic mobile radio channels, free space propagation does not apply. We use a general propagation model that has been accepted widely [30]. A parameter α is used to denote the power law relationship between distance and received power. As a function of distance d , the path loss (in decibels) is expressed as

$$L(d) = 10\alpha \log(d) + S_\sigma(d) \tag{3.1}$$

where $\alpha = 4$ is the propagation coefficient and $S_\sigma(d)$ is shadow fading factor which is a zero mean Gaussian random process along the distance d (with units of dB) with a standard deviation of $\sigma = 6dB$.

The autocorrelation of the shadow fading process is a modeled as in [24].

$$R_{S_\sigma}(\Delta d) = \sigma^2 e^{-\Delta d/D} \tag{3.2}$$

where Δd is the distance between two points and $D = 50$ meters is the shadow fading correlation distance.

3.2 Two Dimensional Microcell

Microcells are attracting much attention because they can accommodate more subscribers per unit service area than macrocells. Also, they permit access by low-power portables. Propagation in microcells differs significantly from that in macrocells. Microcells cannot be simulated by merely changing the scale of the spatial extent of the cells. With a cell size of a few hundred meters, traffic cannot be assumed to be uniformly distributed. Instead road structures have to be considered. This, on one hand, has a strong influence on the mobility model.

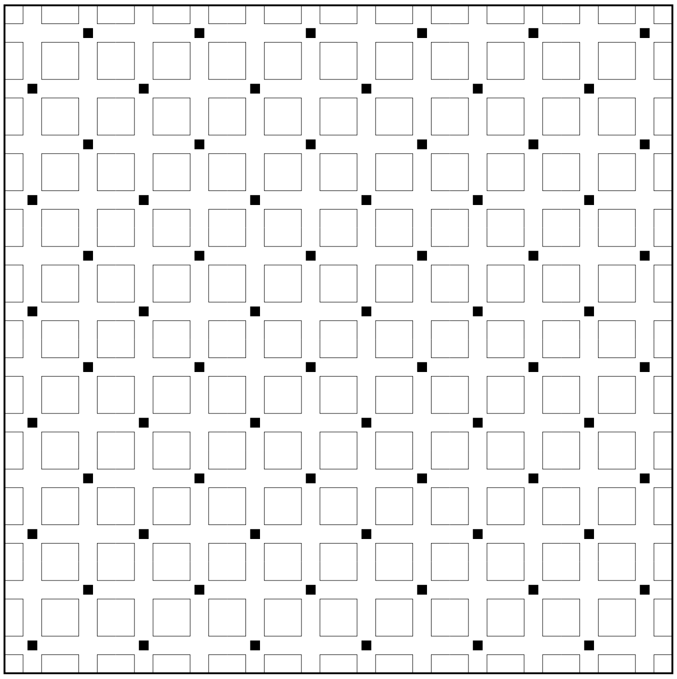

Figure 3.1: Manhattan model for 2-Dimensional Microcells

As depicted in Figure 3.1, we assume Manhattan-like road grid structure which is formed into torus-like structure in order to avoid edge effects. The size of the map is 12 blocks by 12 blocks with block size 200m. Base stations are located on every other intersection, at the height of a lamp post. This results in cells in the shape of "+". This is only a special case. The number of streets between may vary. Also the position of base stations in the middle of the streets may be possible.

Free flowing traffic with a truncated Gaussian speed distribution is assumed with mean value of 40km/hr and standard deviation of 15km/hr, truncated at a minimum speed of 10km/hr and a maximum speed of 70km/hr ($\pm 2\sigma$ points). Traffic is allowed only along the streets. The new call arrivals are uniformly distributed on all the streets and the two directions along the street are equally likely. Although for each call, the speed is assumed to remain constant, the mobile turns left or right or goes straight with certain probabilities at every junction.

Propagation Model

Infinitely high buildings are assumed and a model that differentiates between line-of-sight (LOS) and non-line-of-sight (NLOS) propagation is applied [21]. The path loss model is dependent on where the transmitter and the receiver are positioned. Assuming that the transmitter is in the origin, we use the coordinates (x, y) to describe the receiver position (Figure 3.2). As seen in the figure, the receiver is on a line of sight street when $y = 0$ and on a non line of sight street otherwise.

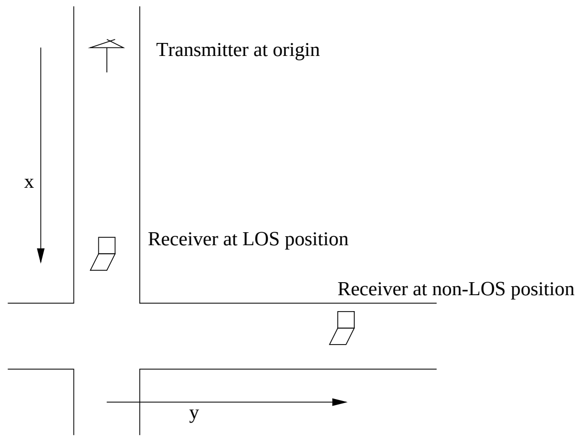

Figure 3.2: Description of the (x,y) coordinates in the path loss model.

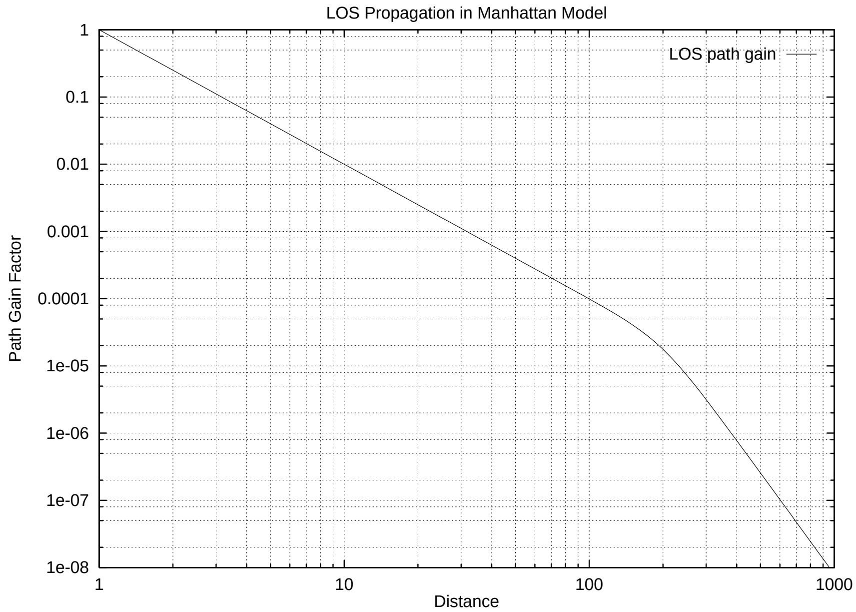

Figure 3.3: Propagation gain factor $P_{\mathrm{LOS}}(x)$ for an MS on LOS path with BS

If the MS is on a line of sight street the received signal power can be modeled as

$$P_{\mathrm{LOS}}(x) = P_t(x^{qp} + x_b^{(q-r)p} x^{rp})^{-\frac{1}{p}} \tag{3.3}$$

where x is the distance from the BS to the MS, $P(x)$ is the received power of the MS at LOS position x, P_t is the BS transmitting power and p, q and r are parameters of the propagation model. q and r are propagation constants describing the "steepness" of the distance attenuation. Figure 3.3 is the path gain on LOS path. As seen in Figure 3.3, we can see a break point at x_b meters from the transmitter. Between the transmitter and x_b the distance attenuation constant is approximately q, whereas beyond x_b the distance attenuation constant is approximately r. The parameter p determines the smoothness of the transition from steepness q to r.

The model for the received signal power if the MS has moved around a corner is

$$P_{\mathrm{NLOS}}(y) = P_{\mathrm{LOS}}(x)((\frac{y}{y_1} + 1)^{qp} + (\frac{y_b}{y_1} + 1)^{qp}(\frac{y + y_1}{y_1 + y_b})^{rp})^{-\frac{1}{p}} \tag{3.4}$$

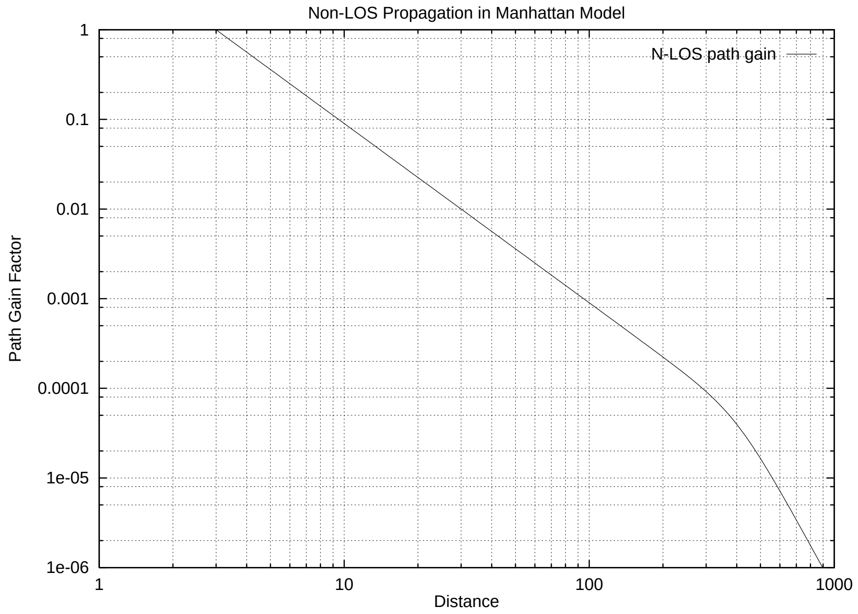

Figure 3.4: Additional path gain factor $P_{\text{NLOS}}(y)$ after the MS turned the corner onto N-LOS path

where y is the distance between the street corner and the receiver. $P_1(x)$ is the power that would be received at the corner if the mobile had been positioned there and $P(y)$ is the received power of the MS at Non-LOS position y meters after the corner. Finally, the parameter y_1 controls the decline just after the corner. The propagation parameters are set as the following: $q = 2$, $r = 5$, $p = 2$, $x_b = 200m$, $y_b = 400m$, $y_1 = 2m$. Figure 3.4 is the additional path gain after the MS turned the corner. We can see that the received signal strength stays the same for a very short distance (2 meters) after the corner because of the reflections near the corner. Then, the received signal strength drops very fast for about 20 dB in 30 meters. Again, there is a break point at y_b.

In addition, shadow fading with a standard deviation of $\sigma = 4dB$ is added to the propagation factors above. The shadow fading has the same autocorrelation function as Equation 3.2 with a much shorter correlation distance $D = 2$ meters [24, 22].

3.3 Two Dimensional Macrocell

We assume the same road grid structure as the two dimensional microcell model but with a much larger size (Fig. 3.5). It is also formed into torus-like structure in order to avoid edge effects. The size of the map is 24 blocks by 24 blocks with block size 500m. Cells are hexagonal with a radius of 1000m. The base stations are located at the center of each cell. The antenna height is 50 meters.

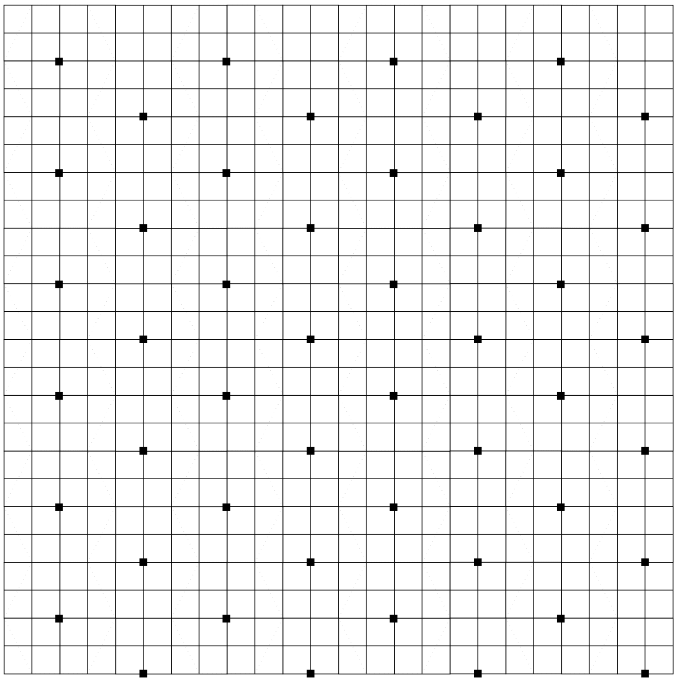

Figure 3.5: Cell Layout model for 2-Dimensional Macrocells

Mobility Model

Free flowing traffic with a truncated Gaussian speed distribution is assumed with mean value of 90km/hr and standard deviation of 15km/hr, truncated at a minimum speed of 60km/hr and a maximum speed of 120km/hr ($\pm 2\sigma$ points). Traffic is allowed only along the roads for simplicity. The new call arrivals are uniformly distributed on all the roads and the two directions along the road are equally likely. Although the speed is assumed to keep constant, the mobile turns left or right or goes straight with certain probability at every junction.

Propagation Model

The propagation model is the same as the one dimensional macrocell, as defined in Equation 3.1. The distance d is defined as the direct distance between the BS and the MS.

3.4 Call Traffic Model

The calls are assumed to arrive according to a Poisson process with intensity λ calls/second, and the call duration is modeled with an exponential distribution with mean μ. The results will be derived as a function of load ρ in Erlang/cell/channel. An average call duration of 120 seconds is used. The newly arrived mobiles are uniformly distributed over all locations.

3.5 Radio channels

Both narrowband FDMA/TDMA and wideband CDMA radio channels can be simulated. Narrowband FDMA/TDMA channels are assumed to be orthogonal, hence mobiles using different channels do not interfere with each other. For TDMA systems, we assume the timing of all the base stations are synchronized. For FDMA/CDMA systems, each wideband channel (frequency) is orthogonal to each other, but more than one MSs could be using the same wideband channel at the same BS and interfere with each other (which is the nature of CDMA system).

We also assume the base stations are constantly sending a pilot tone signal at a certain constant power P_c which is known to all the mobiles.

Chapter 4
Simulation Program

A simulation tool called Mobility And Dynamic Resource Allocation Simulator (MADRAS) has been previously developed at WINLAB to investigate effects of mobility on radio resource management. The simulator is written in C and consists of different modules that can be replaced to investigate different resource management schemes. The MADRAS simulator can only simulate one dimensional macrocellular TDMA/FDMA systems with fixed base station location and cell size.

In this work, a more powerful simulator (MADRAS V3) is developed. It is capable of simulating both one dimensional and two dimensional, both macrocell and microcell, both narrowband (TDMA/FDMA) and wideband (CDMA) systems. The positions and number of base stations can be configured flexibly through a base station configuration input file. All the other configurations can also be changed easily through a parameter input file.

4.1 Program Structure

MADRAS V3 is a discrete event driven simulation program. New events are generated during the simulation and inserted into an event queue according its event time. The event at the head of the queue, which is the event with the earliest event time in the queue, is alway dealt with by the program. After the first event is processed, it is removed from the queue, so the next event in the event queue becomes the head of the queue and will be processed next.

Different events have different tasks during their processing according to their different event types. There are two general event categories in MADRAS V3, namely the global event and the mobile event.

The global events include two event types which have impact on the whole system. They are `GlobalPositionUpdate` and `GlobalStaticsCollection`. The mobile events only happen to a mobile. These events are called `MobileArrival`, `MobileResourceMgnt`, `MobileReachJunction` and `MobileDeparture`.

4.1.1 Global Events

`GlobalPositionUpdate`

At the simulation initialization, a `GlobalPositionUpdate` event is scheduled at the beginning of the simulation. Each time a `GlobalPositionUpdate` event is processed, it calculates the new positions of all the active mobiles according to their old positions, speeds and directions, and updates the positions. It also schedules the next `GlobalPositionUpdate` event at certain time (`PositionUpdateTimeInterval`) later.

`GlobalStatisticsCollection`

At the simulation initialization, a `GlobalStatisticsCollection` event is scheduled at the beginning of the main simulation phase, which is explained later in Section 4.5. Each time a `GlobalStatisticsCollection` event is processed, the SIRs and the powers of both the uplink and the downlink of all the active mobiles in the system are recorded. It also schedules the next `GlobalStatisticsCollection` event at certain time (`StaticsCollectionTimeInterval`) later. Using the statistics collected in this event, histogram tables can be generated at the end of the simulation.

4.1.2 Mobile Events

All the following events only happen to a particular mobile whose index number is part of the data structure of these events.

`MobileArrival`

At the simulation initialization, a `MobileArrival` event of mobile No.1 is scheduled at the beginning of the simulation. Each time a `MobileArrival` event is processed, the admission control policy checks whether to admit this new mobile. If the new mobile is admitted, several new events will be scheduled for this new mobile. A `MobileDeparture` event is scheduled at the mobile's departure time. A `MobileResourceMngt` event is scheduled at certain time (`ResourceMngtTimeInteval`) later. A `MobileReachJunction` event is scheduled at certain time later according to the new mobile's location, direction and speed. Whether the new mobile is admitted or not, a `MobileArrival` event for the next new mobile is scheduled to occur after an exponentially distributed time with a mean of `AverageCallDuration` seconds.

`MobileResourceMgnt`

The `MobileResourceMgnt` event performs the radio resource management task on the corresponding mobile. It adjusts the transmit powers of both uplink and downlink based on the current measurement of the SIR level and the current transmit power. It also checks the radio link quality to decide whether a handoff should be initiated. When the handoff condition is satisfied, it tries to make a handoff for the mobile. Sometimes if the radio link is too bad, it may also drop the call. If the mobile is still active (not dropped) at the end of this event, a next `MobileResourceMgnt` event will be scheduled at a certain time (`ResourceMngtTimeInteval`) later.

`MobileReachJunction`

The `MobileReachJunction` event updates the position of the mobile and changes the direction of the mobile with a specified probability. It will also schedule the next `MobileReachJunction` event to occur after certain time which depends on the mobile speed and the block size.

4.2 Basic Data Structures

Event Structures

The event structures form a queue which is implemented using a bidirectional linked list. Each of the event structure consists of:

`EventType` and `EventTime`: type and time of the event.

`MobileIndex` and `MobilePointer`: the corresponding mobile index and pointer to its data structure if the event is one of the mobile events.

Mobile Station Structure

The mobile station structure is kept in a linked list. The fields of the MS structure are:

`Index`: mobile identification number.

`ArrivalTime` & `DepartureTime`: time of call arrival and departure.

`x, y`: position of the terminal.

`xyPointer`: pointer to the structure of a geographical point, which contains the array of path gain factors from the point to each base station.

`PosTime`: exact time of this mobile reaching its current recorded position `(x,y)`.

`Direction` & `Speed`: direction and speed of the mobile.

`Channel` & `Base`: channel and base station assigned to this mobile.

`UpPower` & `DnPower`: uplink power transmitted by the mobile and downlink power transmitted by its base station to the mobile.

Base station

The base station information is stored in an array of structures. Each base station structure contains the following fields:

`Color`: the channel set used in fixed channel assignment if applicable.

`x, y`: position of the base station.

`NumberOfMobile`: number of mobiles in this cell.

`ChannelAvail[]`: array of flags indicating the availability of channels at this base in FCA.

`PointerMobile[]`: array of pointers to linked lists for the mobiles using each channel in this cell.

`NoMobile[]`: array of the numbers of mobiles using each channel. In FDMA/TDMA systems, at most one MS can be using one channel, but in FDMA/CDMA systems, each channel is normally used by more than one MS at a BS.

The positions and the colors of the base stations are set by the user in the base station configuration file. This gives the user a lot of flexibility in simulating different systems.

Geographical Model and the Path Gain

The data structure for the geographical model should also provide a easy way to implement the mobility model and contain the path gain information. A data structure for a geographical point is defined as the following

`PathGainToBase[B]`: array of the path gain factors from each base station to this point. `B` is the number of BSs in the system.

`StrngstBase`: the base station with the highest gain from this point.

At the initiation of the simulation, a point structure is generated every `DistRes` (which is a global variable) meters along the streets and the avenues and these point structures are organized into two 2-dimension arrays. The path gain factors are all pre-calculated and the shadow fading is added. Later in the simulation, the path gain from a mobile to a BS can be obtained from the mobile's position and hence the pointer to the point structure.

4.3 Some Key Parameters

Almost all the simulation parameters are global variables and have default values, which can also be changed by the parameter input file. These adjustable parameters include:

`DistRes`: the distance resolution between two consecutive point structures. Because of the limited memory in a computer, we cannot generated a infinitely detailed map of the cell layout. We can only sample the map with certain distance resolution and generate a geographical point data structure every `DistRes` meters.

`NoBase`: number of base stations in the system.

`NoChnl`: total number of channels in the system.

`NoisePwr`: noise power.

`MaxPwr`: maximum transmit power of the mobiles and the base stations.

`MeanSpeed, MinSpeed, MaxSpeed, SigmaSpeed`: speed distribution parameters.

`ProbAhead`: probability of going straight ahead at a junction (not applicable for 1-dimensional system).

`PosTmRes`: time between position update events.

`SirTmStep`: time between statistics collection events.

`RsrcTmStep`: time between resource management events.

The parameters used in three simulation models are listed in Table 4.1. In some experiments, some parameters will be set different from these tables. these different parameters will be stated when explaining the experiments in the next chapter.

Table 4.1: Simulation Parameters

Parameters	1D	2D Micro	2D Macro
Number of BSs	20	72	48
Number of Channels	40	40	40
Cell Radius (m)	1000	200	1000
Antenna Height (m)	50	10	50
Distance Resolution (m)	1	5	5
Shadow Fading Standard Deviation (dB)	6	4	6
Shadow Fading Correlation Distance (m)	50	2	50
Noise Power (dBW)	-150	-150	-150
Maximum Power (dBW)	0	0	0
Mean Speed (km/hr)	90	40	90
Maximum Speed (km/hr)	120	70	120
Minimum Speed (km/hr)	60	10	60
Standard Deviation of Speed (km/hr)	15	15	15
Probability of Going Straight	N/A	0.6	0.6
Time Between Position Updates (Second)	0.5	0.5	0.5
Time Between Statistics Collection	1	1	1
Time Between Resource Management Events	1	1	1
Target SIR γ_{t} (dB)	20	20	20
Drop SIR γ_{floor} (dB)	14	14	14
Admission SIR γ_{new} (dB)	23	23	23

4.4 Performance Measures

The output of the simulation program MADRAS V3 consists of a detailed log of every power adjustment, admission and handoff, histograms of SIR, transmit power and handoff distance distribution. It also gives out some important system performance measures including the new call blocking probability, P_{b}, the ongoing call dropping probability, P_{d}, and the handoff failure probability, P_{hf}, which can be estimated as the following

$$P_{\mathrm{b}} = \frac{\text{blocked new calls}}{\text{call arrivals}} \tag{4.1}$$

$$P_{\mathrm{d}} = \frac{\text{dropped calls}}{\text{accepted calls}} \tag{4.2}$$

$$P_{\mathrm{hf}} = \frac{\text{handoff failures}}{\text{handoff attempts}} \tag{4.3}$$

and average handoff distance and average number of handoffs per call.

4.5 Simulation Process

At the begin of each simulation, a set of simulation parameters are read into the memory from a parameter input file. Then the program enters the initialization phase, where the corresponding street model, cell layout and propagation path loss factors are established or calculated. The first `GlobalPositionUpdate` event and the `MobileArrival` event of MS No.1 are scheduled at the beginning of the simulation, at system time 0.

After the initialization phase, the program enters the start-up phase, where the program generates additional events during the processing of the current events according to the logic of each event. In particular, the program generates other `MobileArrival` events according to Poison arrival model. As the system clock advances, more and more MSs arrive, are admitted (or blocked), move around, while continually performing power control and occasionally handoff. The start-up phase time is set long enough (10 minutes) for the system to achieve steady state.

After the system clock passes the start-up phase time, the program enters the steady state — the main simulation phase. The first `GlobalStaticsCollection` event is scheduled at the beginning of this phase. Basically the program is doing the same thing as in the start-up phase. The difference is that the `GlobalStaticsCollection` event starts to happen only in the main simulation phase, so that the statistics collected are accurate.

When the system clock passes the length of the main simulation phase, which is normally set to 10 hours, the program stops the simulation loop and presents the statistics.

Chapter 5
Simulation Results and Analysis

MADRAS V3 is a very flexible simulation tool making it possible investigate a wide range of issues related to radio resource allocation. In this chapter, we give a few examples which characterize the effect on several performance measures of: channel allocation and admission control techniques (Section 5.1), handoff strategies (Sections 5.2 and 5.3), dynamics of power control (Section 5.4), and system capacity (Section 5.5). These examples are chosen to demonstrate the variety of issues that can be addressed with MADRAS V3.

5.1 Performance of ACP-DCA Admission Control

Figures 5.1, 5.2 and 5.3 show the blocking probability vs. the offered traffic in three different simulation models. Figures 5.4, 5.5 and 5.6 show the dropping probability vs. the offered traffic in the three simulation models. These experimental results are for the SIR admission threshold/LI-DCA and the ACP-DCA admission control schemes with different SIR admission thresholds, γ_{new}.

We find that the dropping probability of ACP-DCA in all three cases is less than the SIR admission threshold/LI-DCA scheme. The cost is that blocking probabilities for ACP-DCA are higher than those of SIR admission threshold/LI-DCA. Thus, the improvement of the dropping probability may have been caused by two factors, one is simply the reduced carried traffic because of the higher blocking probability, the other is the selective rejection of those MSs who, if admitted, might cause other active MSs to be dropped. In order to isolate the

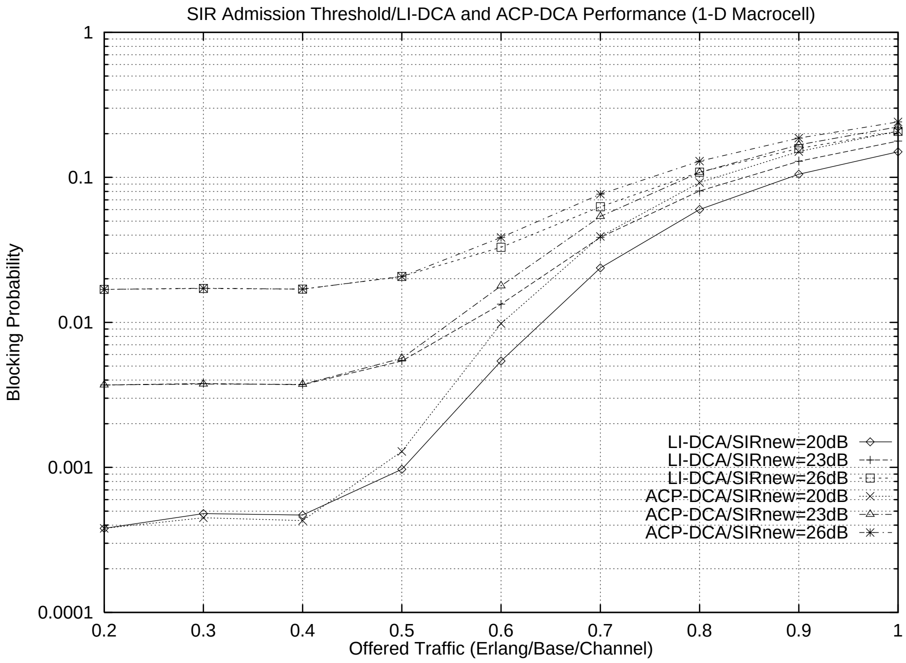

Figure 5.1: Blocking Rate of SIR admission threshold/LI-DCA and ACP-DCA (1-D Macrocell)

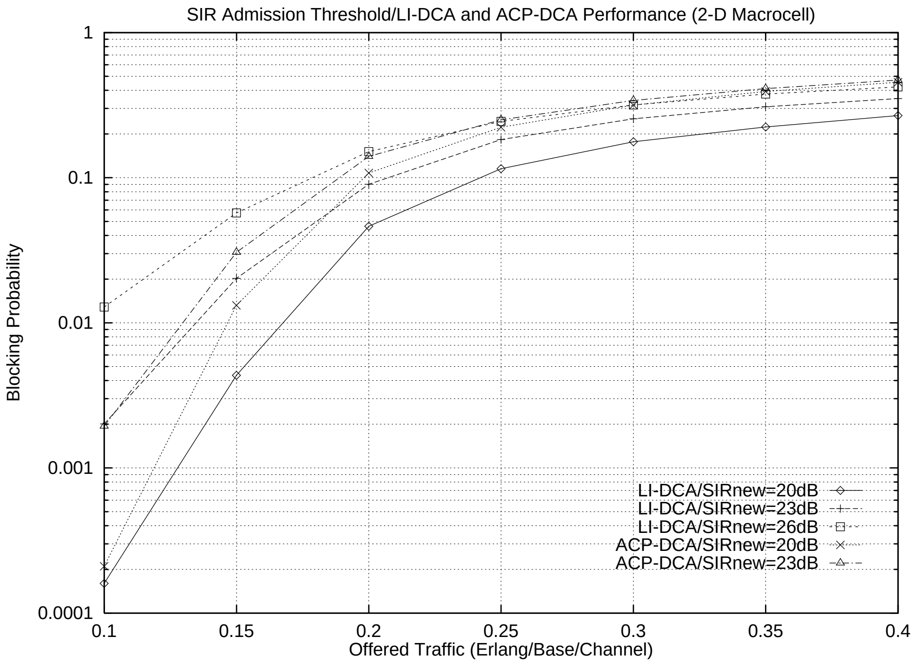

Figure 5.2: Blocking Rate of SIR admission threshold/LI-DCA and ACP-DCA (2-D Macrocell)

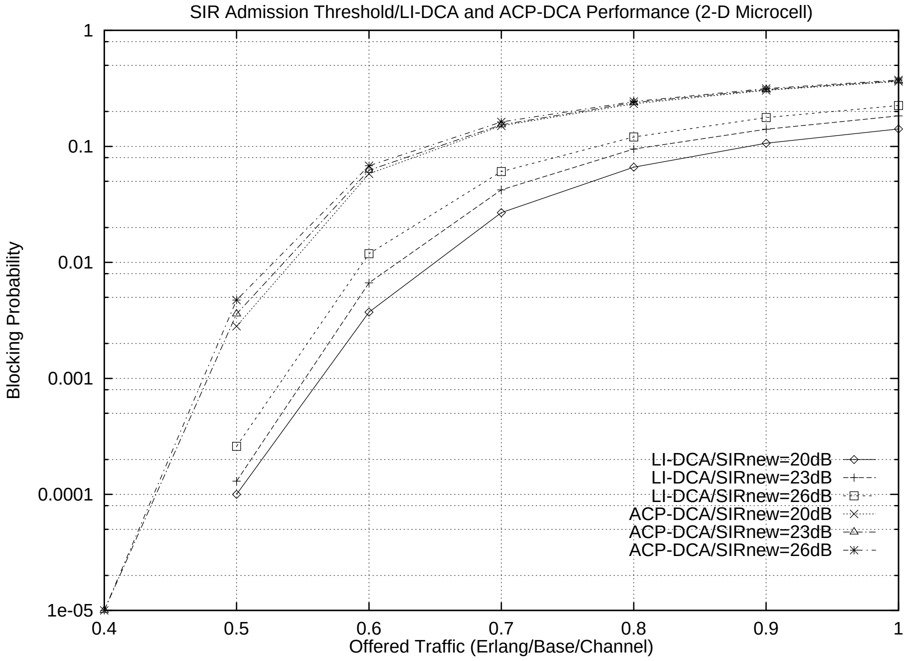

Figure 5.3: Blocking Rate of SIR admission threshold/LI-DCA and ACP-DCA (2-D Microcell)

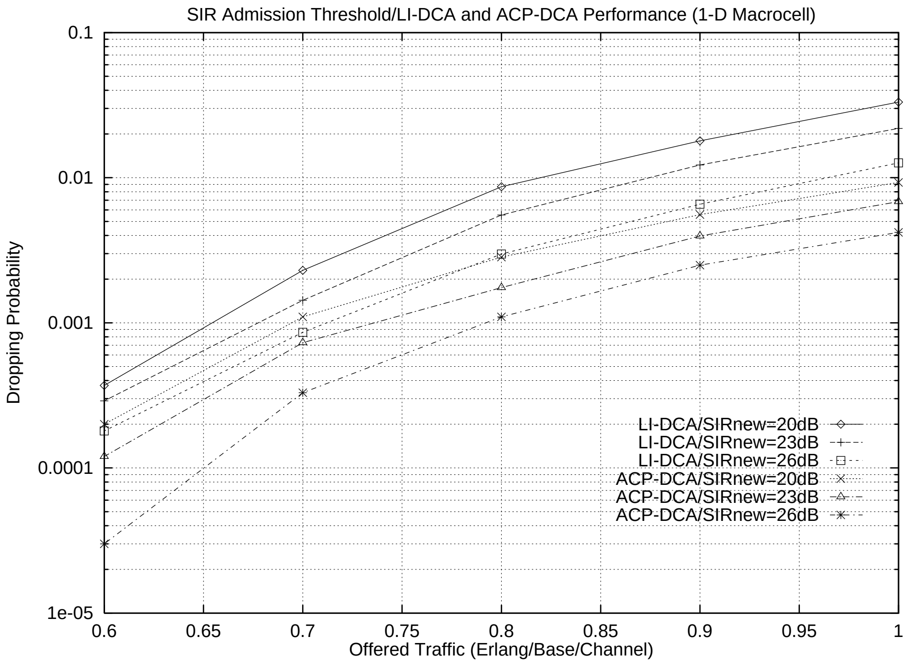

Figure 5.4: Dropping Rate of SIR admission threshold/LI-DCA and ACP-DCA (1-D Macrocell)

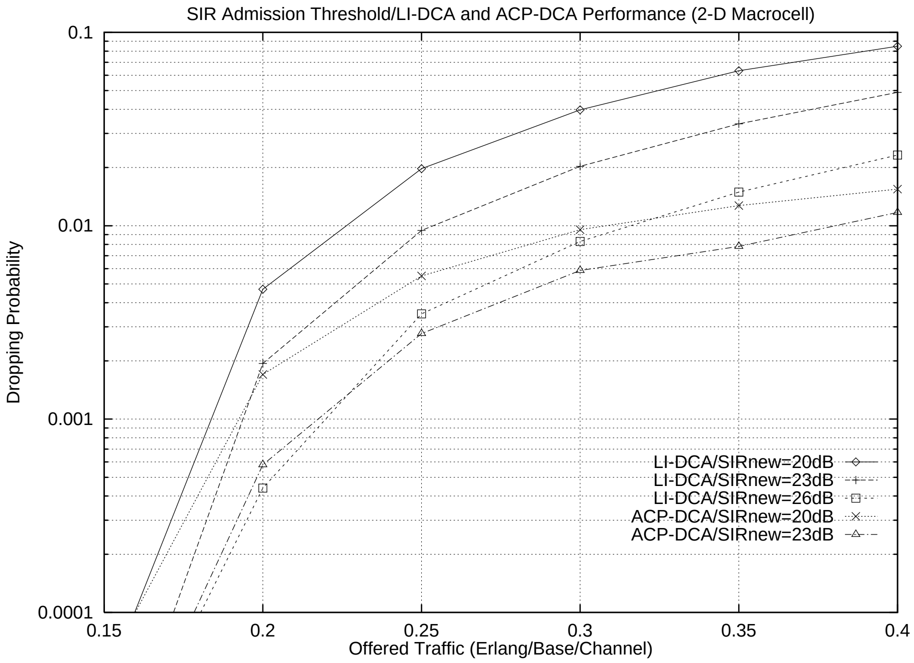

Figure 5.5: Dropping Rate of SIR admission threshold/LI-DCA and ACP-DCA (2-D Macrocell)

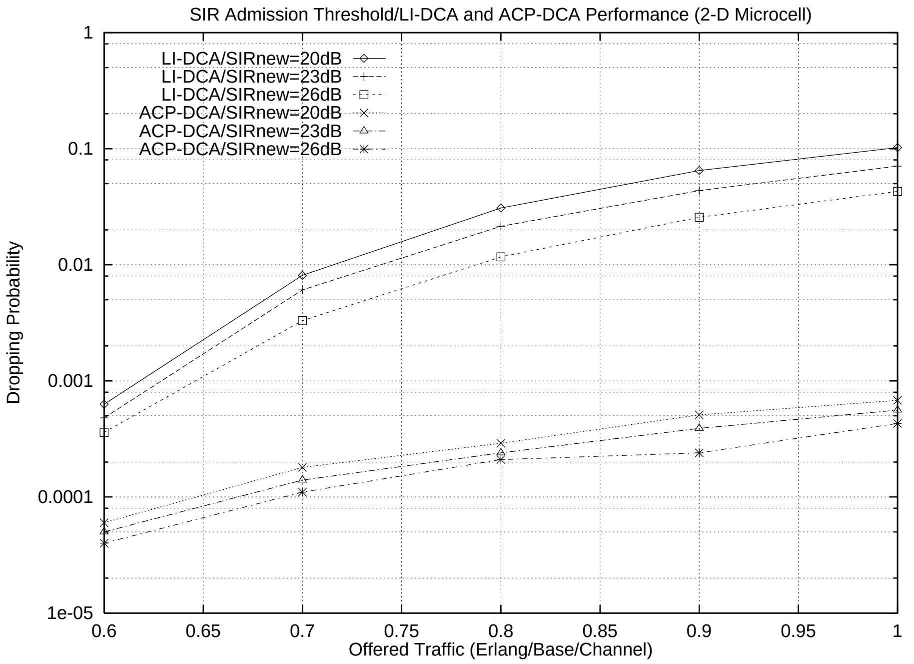

Figure 5.6: Dropping Rate of SIR admission threshold/LI-DCA and ACP-DCA (2-D Microcell)

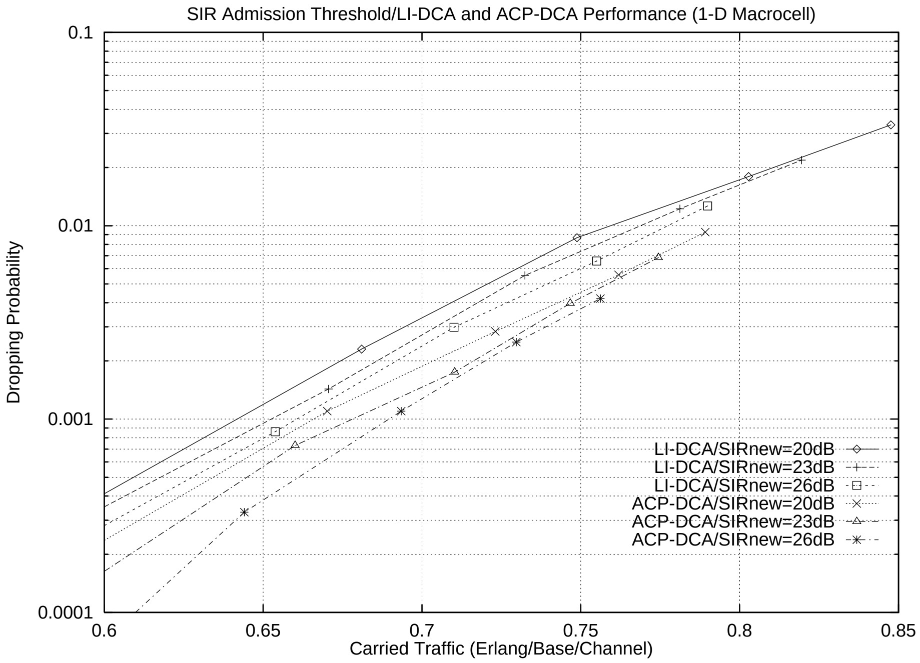

Figure 5.7: Dropping Rate vs. Carried Traffic for SIR admission threshold/LI-DCA and ACP-DCA (1-D Macrocell)

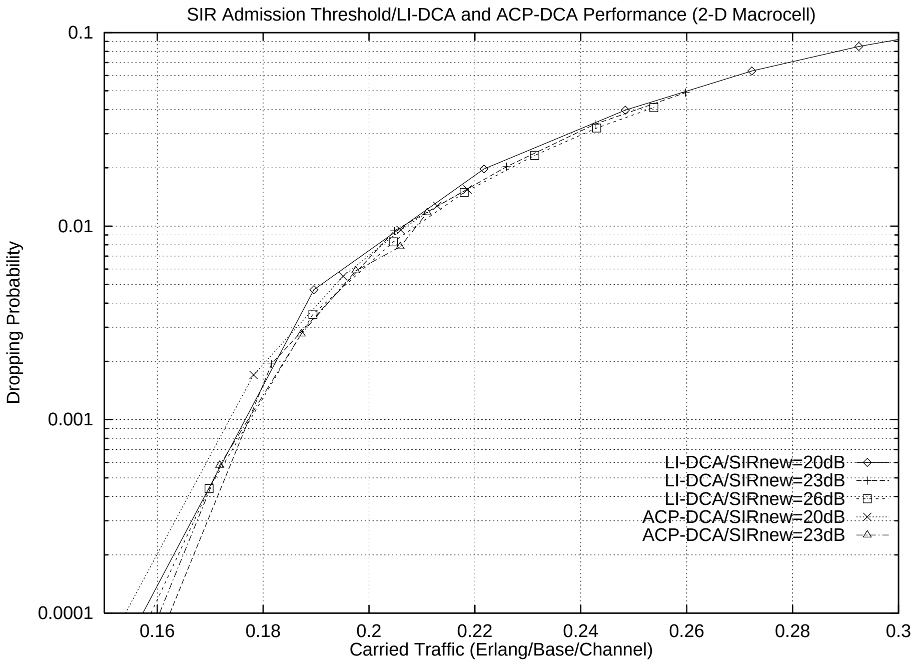

Figure 5.8: Dropping Rate vs. Carried Traffic for SIR admission threshold/LI-DCA and ACP-DCA (2-D Macrocell)

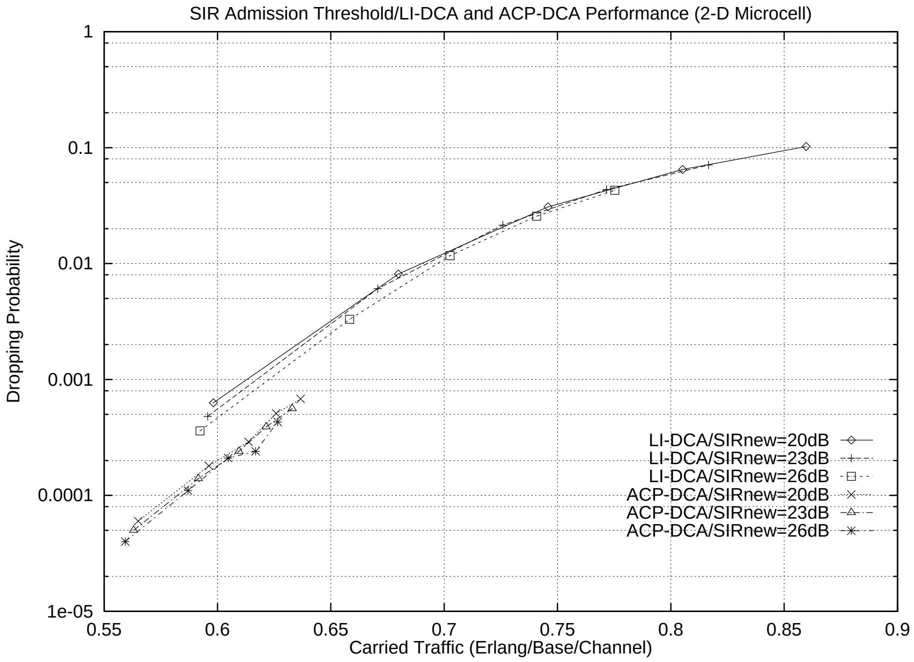

Figure 5.9: Dropping Rate vs. Carried Traffic for SIR admission threshold/LI-DCA and ACP-DCA (2-D Microcell)

second factor, we plot the dropping probability vs. the carried traffic, as shown in Figures 5.7, 5.8 and 5.9. From these figures, we see that the improvement in dropping probability of ACP-DCA over SIR admission threshold/LI-DCA is very small in the 1-dimensional and 2-dimensional microcell cases. There is almost no improvement in the 2-dimensional macrocell case.

It should be noted that in the dropping probability plots of Figure 5.9, the range of offered traffic for the ACP-DCA schemes is small because of the high blocking rate of the ACP-DCA schemes in the 2-D microcell case. For example, we see from Figure 5.3 that an offered traffic of 1 Erlang/Base/Channel yields a blocking rate of the ACP-DCA schemes of approximately 0.35, and so the carried traffic is reduced to 0.65 Erlang/Base/Channel.

We also find, for both SIR admission threshold/LI-DCA and ACP-DCA schemes, that higher γ_{new} causes higher blocking and hence lower dropping. But from Figures 5.7, 5.8 and 5.9 for the dropping rate vs. carried traffic, we find that higher

γ_{new} helps very little in protecting active channels. In particular, ACP-DCA offers no improvement over SIR admission threshold/LI-DCA in the 2-dimensional macrocell case. Thus, we can conclude that the small performance improvements of ACP-DCA over SIR admission threshold/LI-DCA do not outweigh the cost of extra information exchange between BSs and MSs required for ACP-DCA.

5.2 Handoff Performance in Macrocells

In this section, we test three distinct handoff algorithms, namely, Received Signal Strength Index based handoff (RSSIBH), SIR based handoff (SIRBH) and Combined RSSI and SIR based handoff (COMBH) (see Section 1.7) in the 1 dimensional macrocell system. Each algorithm was tested with varying parameters. In each simulation, the system is performing ADCPC and LI-DCA with an admission SIR threshold γ_{new} of 23dB. When the corresponding Hand-out Policy is satisfied, LI-DCA is used with a certain Hand-in SIR criteria to allocate a channel to the handoff calls. For the SIRBH scheme, the hand-in SIR criteria is $\gamma_{\text{old}} + H_{\text{hf}}$, where γ_{old} is SIR just before the handoff, and $H_{\text{hf}} = 3\text{dB}$ is the handoff SIR hysteresis. For RSSIBH and COMBH schemes, the Hand-in SIR criteria is just the target SIR γ_{t}.

Figures 5.10, 5.11 5.12, 5.13, 5.14 and 5.15 give handoff performance figures for the 1-dimensional macrocell system. Figure 5.10 shows the average handoff distance vs. carried traffic. Figure 5.11 yields the average number of handoff attempts vs. carried traffic. Figure 5.12 gives the average number of handoffs vs. carried traffic. Figure 5.13 is the handoff failure rate vs. carried traffic. Figure 5.14 shows the dropping rate vs. the carried traffic. Figure 5.15 characterizes the average MS transmit power vs. the carried traffic.

From Figures 5.10 and 5.11, we can see that the handoff distance and the average number of handoff attempts per call of the MSs in the RSSIBH scheme

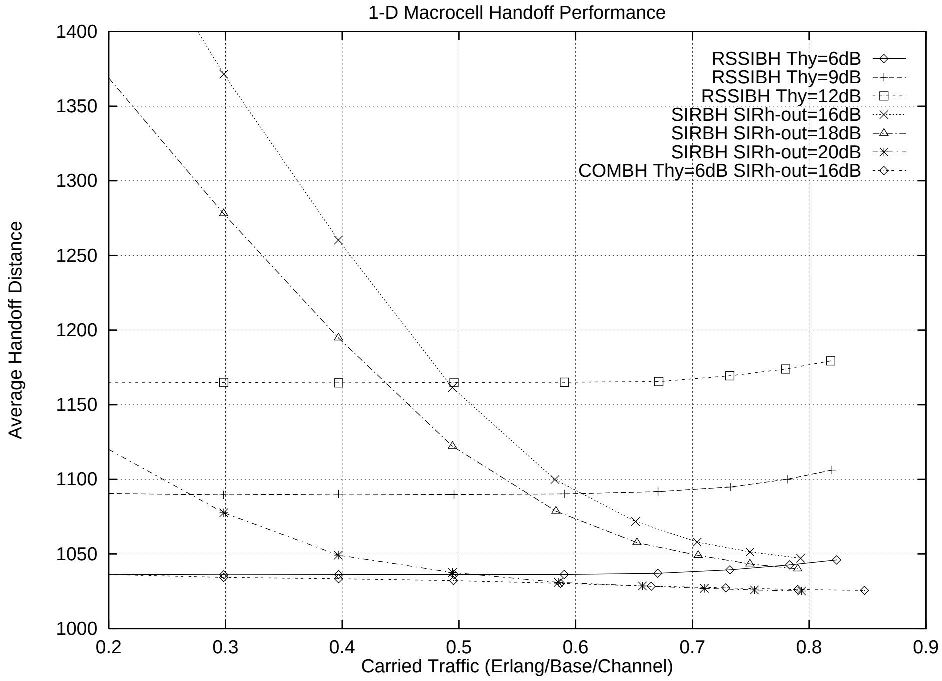

Figure 5.10: Average Handoff Distance of 1-D Macrocell

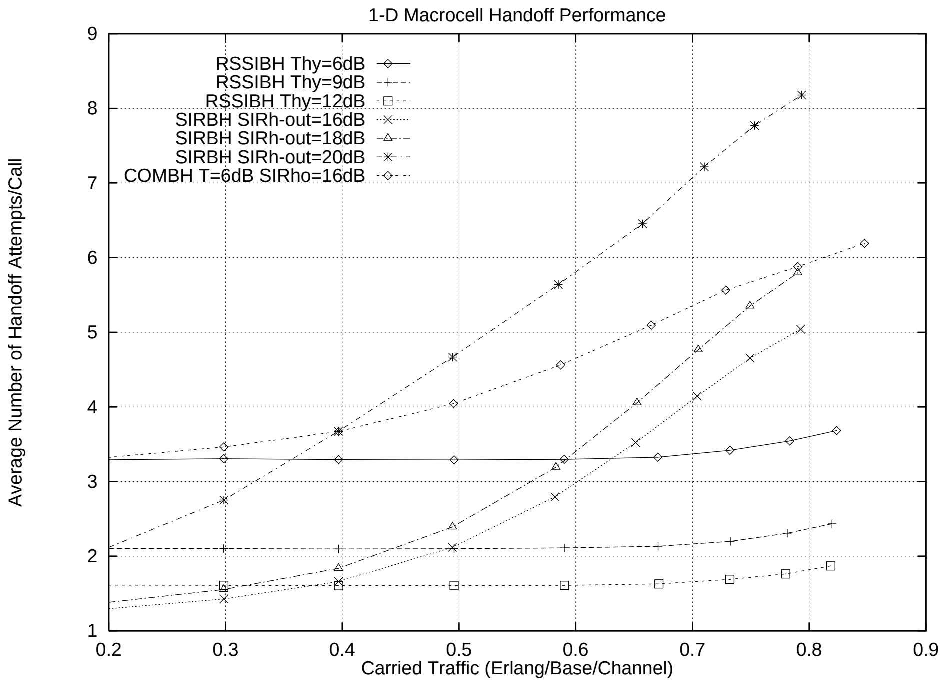

Figure 5.11: Average Number of Handoff Attempts Per Call of 1-D Macrocell

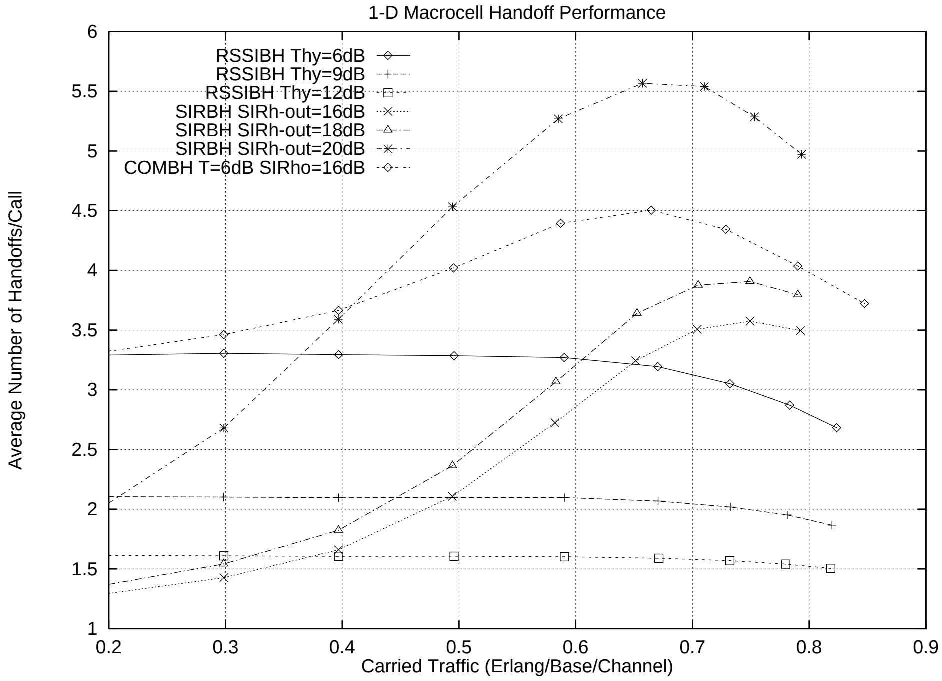

Figure 5.12: Average Number of Handoffs Per Call of 1-D Macrocell

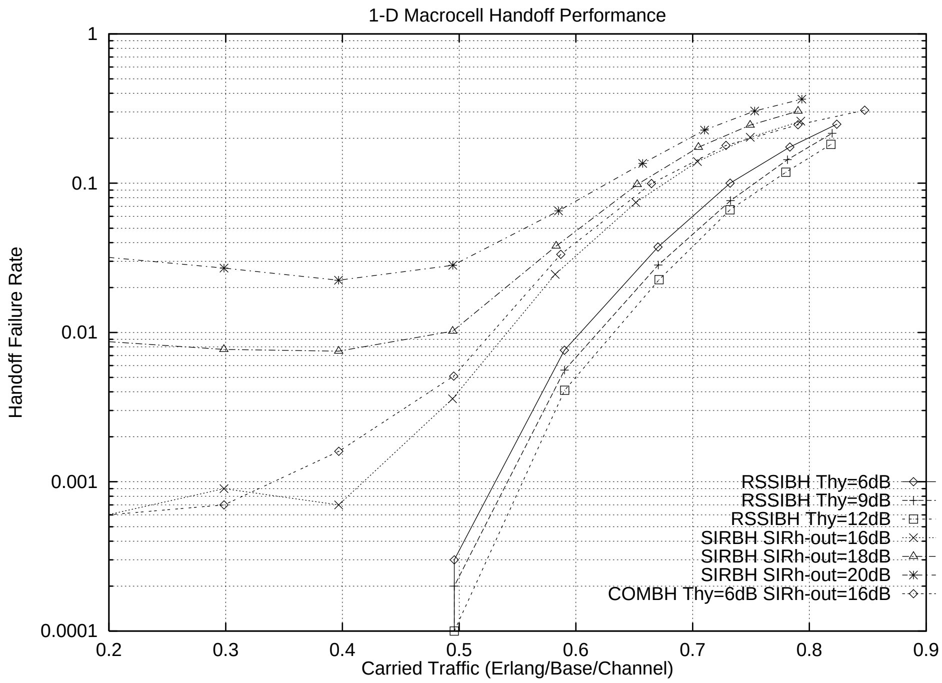

Figure 5.13: Average Handoff Failure Rate of 1-D Macrocell

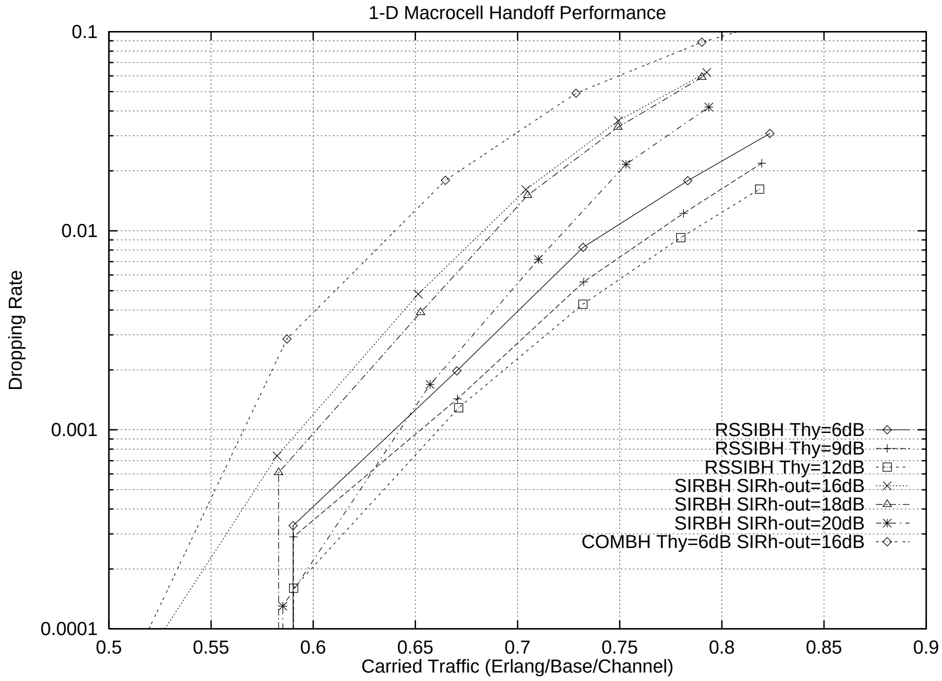

Figure 5.14: Dropping Rate of 1-D Macrocell

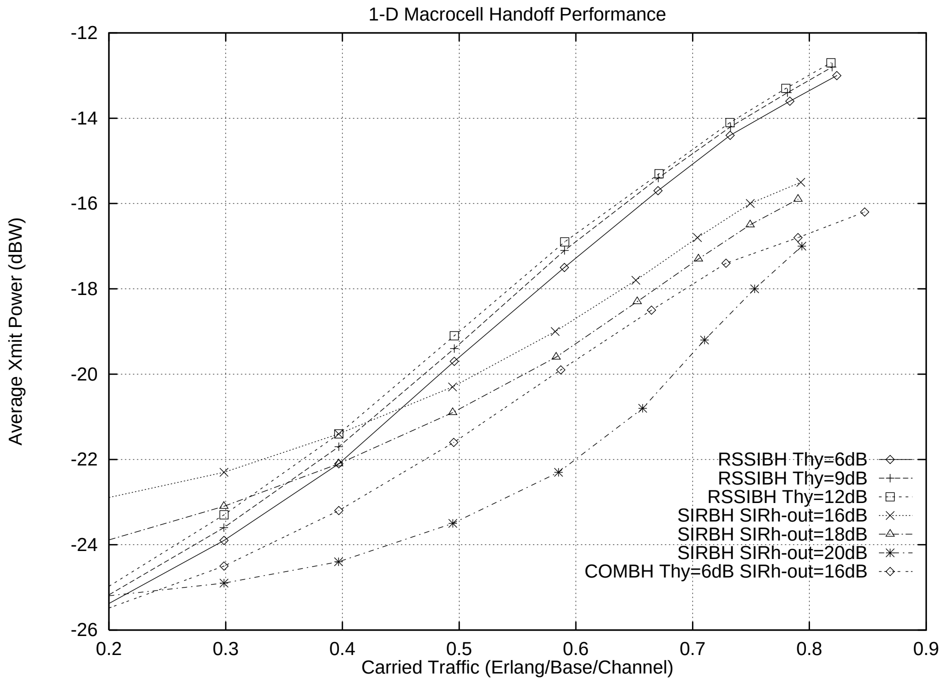

Figure 5.15: Average Transmit Power of 1-D Macrocell

hardly changes when the traffic increases. This is because this handoff scheme uses only the path loss information in making handoff decisions, and thus it is hardly affected by the traffic density. However, the average number of handoff attempts per call does increase a little at high load because the handoff failure rate is very high at high load, as we can see in Figure 5.13. In this case, the MSs have to make more handoff attempts before a successful handoff. Also from Figure 5.12 the average number of handoffs per call in RSSIBH scheme decreases at high traffic load. This is caused by the higher handoff failure rate and dropping rate at the higher traffic density. Most (if not all) of the dropped calls happened near the cell boundary, where the calls are dropped after failed handoff attempts, thus reducing the average number of successful handoffs per call. For an average call duration of 120 seconds and an average MS speed of 90km/hr, each MS typically travels through 1.5 cells during a call. From Figure 5.12, for example, the average number of handoffs per call for RSSIBH with hysteresis $T_{\mathrm{hy}} = 9$dB at low load is 2.1, yielding 1.4 handoffs per call per traveled cell. This result is consistent with [42, 50].

As we expected, we also find that small RSSI hysteresis T_{hy} leads to more handoffs back and forth between the two BSs (the Ping-Pong effect) and a smaller average handoff distance because handoffs happens earlier and more often. Larger RSSI hysteresis leads to later and fewer handoffs, hence the average handoff distance tends to be larger. From Figures 5.13, 5.14 and 5.15 we can see the handoff failure rate, the dropping rate and the average MS transmit power increase as the system becomes more congested. Because larger RSSI hysteresis T_{hy} leads to later handoffs, when a MS attempts to to handoff to another BS, it is normally closer to that BS, so the chance of a successful handoff is also higher, and the handoff failure rate for larger RSSI hysteresis is lower. For the same reason, we can see that larger RSSI hysteresis leads to a little higher average transmit power and lower dropping rate.

From Figure 5.10, we find that the average handoff distance of the SIRBH scheme is extremely high, for hand-out SIR threshold of 16dB and 18dB under low load. This is because by increasing the transmit power, the MS can maintain an SIR above the hand-out SIR threshold even if it is deep inside the new cell. This phenomenon is referred to as cell-dragging. This distance tends to decrease when the traffic increases because the interference received by the MS also increases.

From Figures 5.11 and 5.12, the average number of handoff attempts and the average number of handoffs per call also increase as the system gets more congested and the overall interference level becomes higher. But at higher load the average number of handoffs decreases a little because of the increasing handoff failure rate and dropping probability. Also, we see that the number of handoffs and handoff attempts increases when the hand-out SIR threshold is higher. This is because the higher the hand-out SIR threshold, the more likely the MS's SIR will be lower than the threshold when the MS is using its maximum power, and hence there will be more handoff attempts and more handoffs.

From Figure 5.13, the handoff failure rate also increases when the hand-out SIR threshold is higher. In this case, there are more handoff attempts but because the SIR hysteresis $H_{\mathrm{hf}} = 3\mathrm{dB}$ is constant, the handoff calls will need to achieve higher hand-in SIR which is more difficult to meet.

From Figure 5.15, we see that under SIRBH the average MS transmit power also increases with the traffic load, and is higher than the RSSIBH scheme under low load. This is due to cell dragging in which the MSs will have to transmit more power when they move deeply into other cells while staying connected with the old BS. With higher load, however, SIRBH has lower average transmit power because there are more handoffs caused by the increasing overall interference level. When a handoff occurs in this case, the MS is allocated a channel with the least interference and hence the MS needs less power to reach the target SIR. When the hand-out SIR threshold increases, the average MS transmit power decreases for the same reason, causing lower overall interference, and hence less call dropping as we can see in Figure 5.14. From Figures 5.13 and 5.14, we can also see that the handoff failure rate and the dropping rate of SIRBH also increase with the load.

As for the COMBH scheme, Figures 5.10, 5.11 and 5.12 show that COMBH has the same average handoff distance and average number of handoffs and attempts as the RSSIBH with the same RSSI threshold under low load. In this case, the overall interference level is low and most of the handoffs are caused by the RSSI threshold instead of the SIR threshold. Furthermore, as the system becomes more congested, the interference level becomes higher, and the SIR threshold causes more handoffs, so the average number of handoffs and handoff attempts increase while the handoff distance decreases.

From Figures 5.15, 5.13 and 5.14, the COMBH has lower average transmit power than both the RSSIBH scheme with the same RSSI threshold and the SIRBH scheme with the same SIR threshold because at the low load, the RSSI threshold will keep the MSs using the strongest BS, thus transmitting lower power, whereas at high load, the SIR threshold will make the MSs to switch BS and channel whenever the interference level of the current channel becomes high. Although the COMBH scheme appears to combine the desirable properties of the RSSIBH and SIRBH algorithms, one inexplicable result remains. In Figure 5.14, we observe that the dropping rate of COMBH is significantly higher than that of either RSSIBH or SIRBH. The reason for this occurrence needs further investigation.

5.3 Handoff Performance in 2-D Microcells

We also have tested these three handoff schemes in 2 dimensional microcellular systems. To evaluate the impact of corner effects in the 2-D microcellular propagation model, we ran two simulations with different parameter settings. In

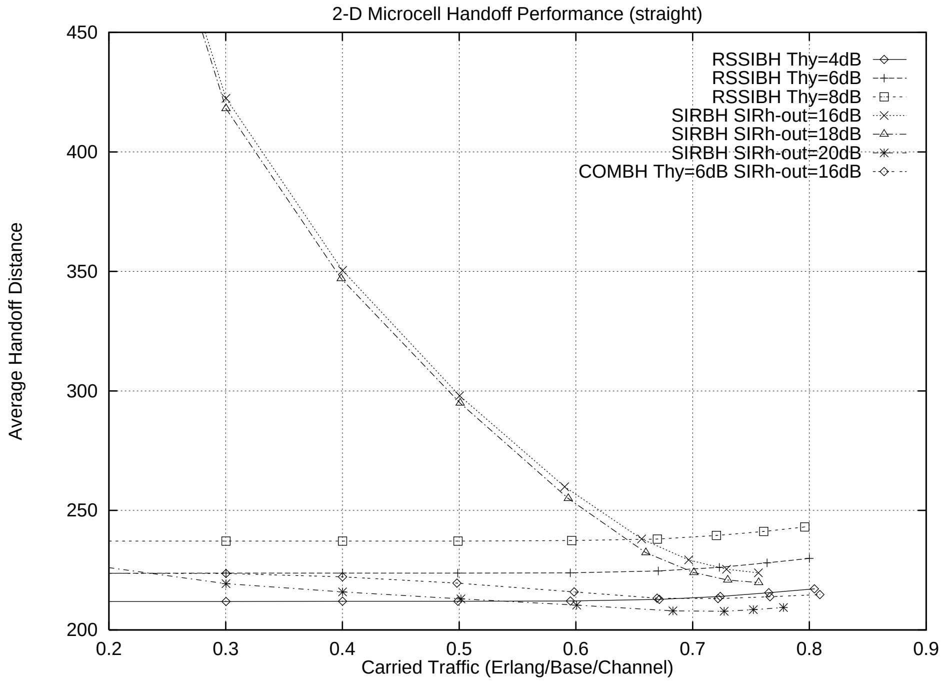

Figure 5.16: Average Handoff Distance of 2-D Microcell (straight)

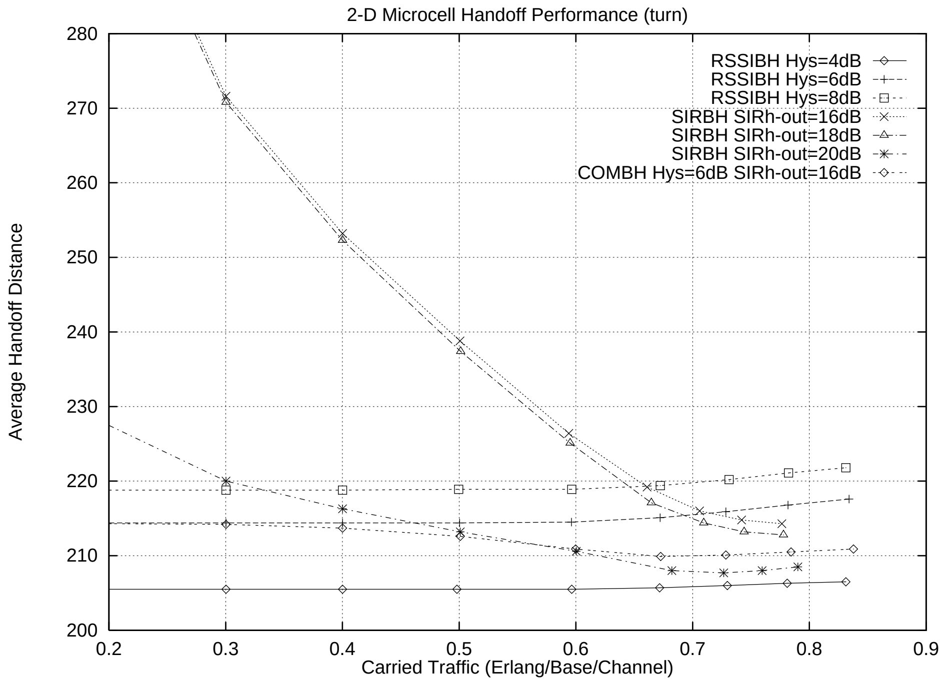

Figure 5.17: Average Handoff Distance of 2-D Microcell (turn)

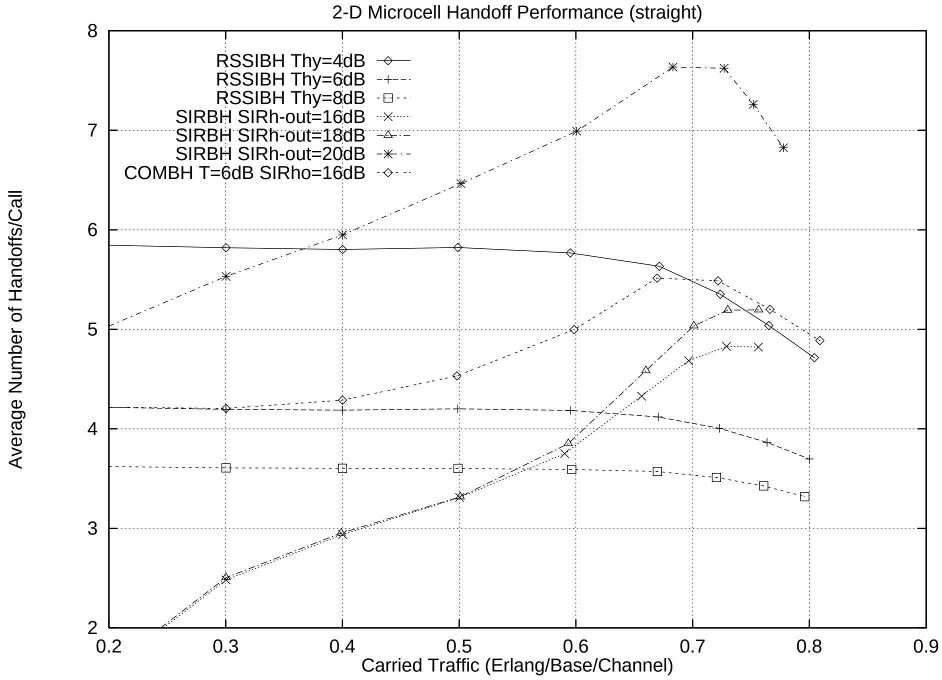

Figure 5.18: Average Number of Handoffs Per Call of 2-D Microcell (straight)

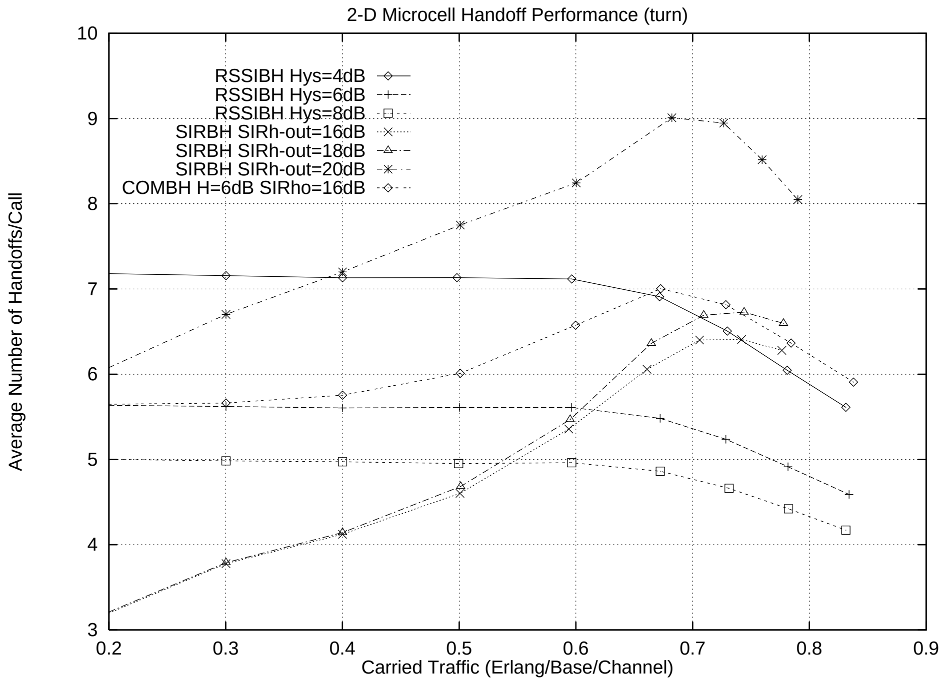

Figure 5.19: Average Number of Handoffs Per Call of 2-D Microcell (turn)

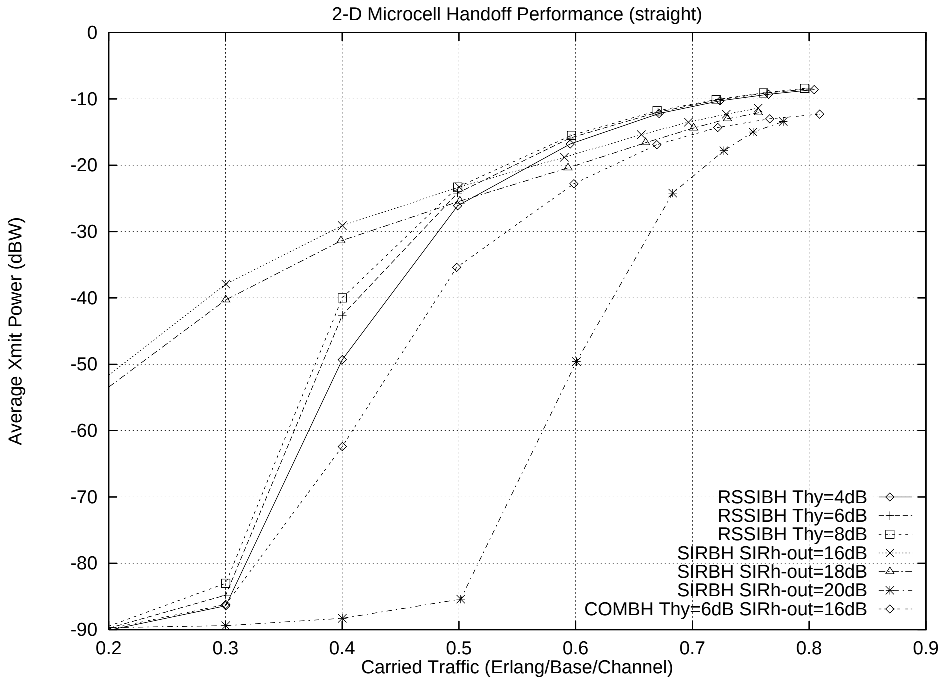

Figure 5.20: Average Transmit Power of 2-D Microcell (straight)

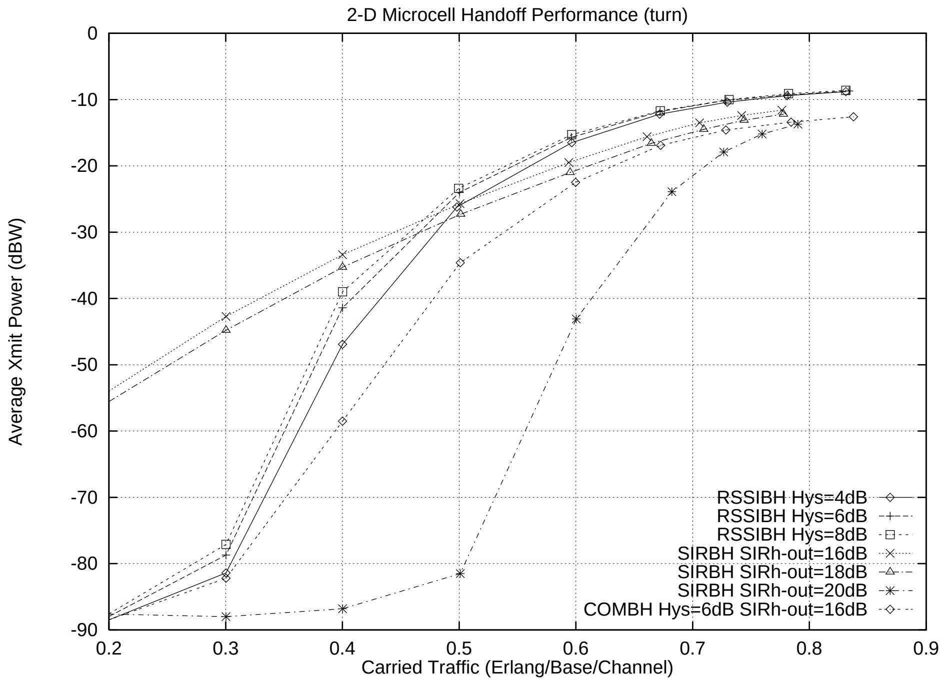

Figure 5.21: Average Transmit Power of 2-D Microcell (turn)

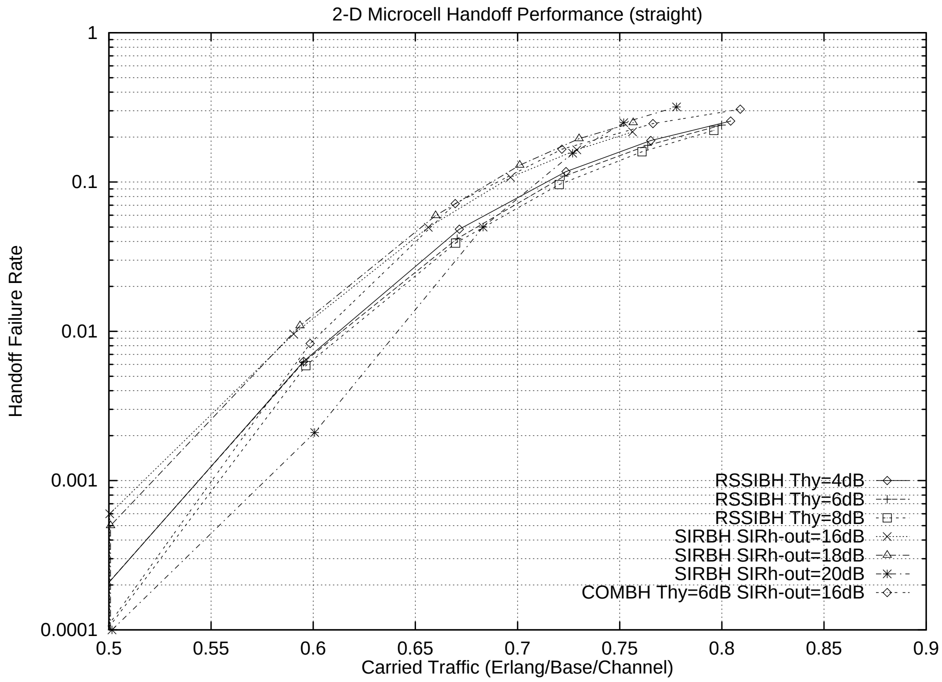

Figure 5.22: Average Handoff Failure Rate of 2-D Microcell (straight)

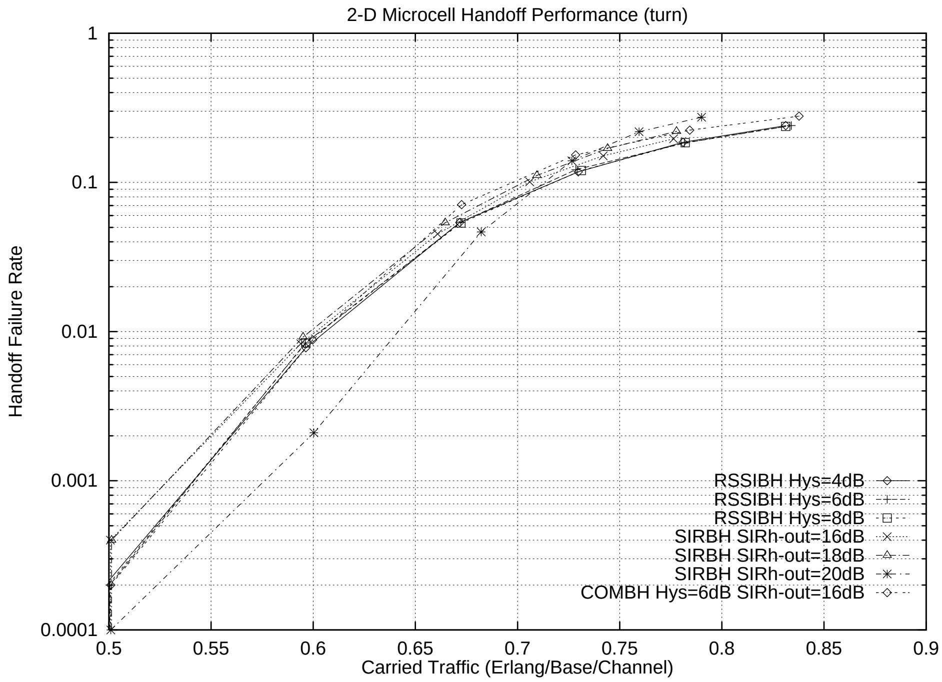

Figure 5.23: Average Handoff Failure Rate of 2-D Microcell (turn)

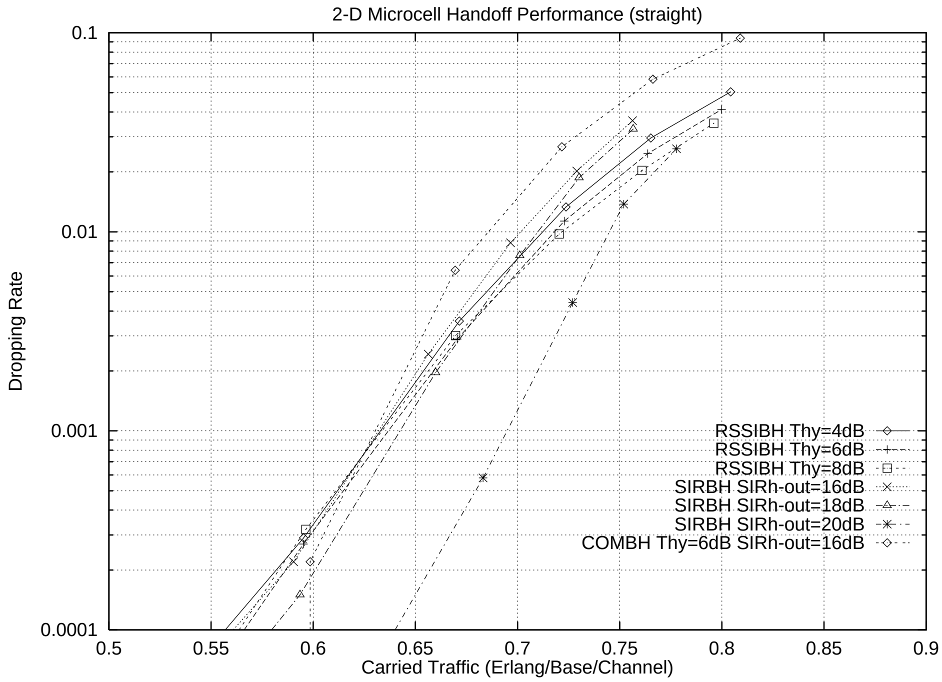

Figure 5.24: Dropping Rate of 2-D Microcell (straight)

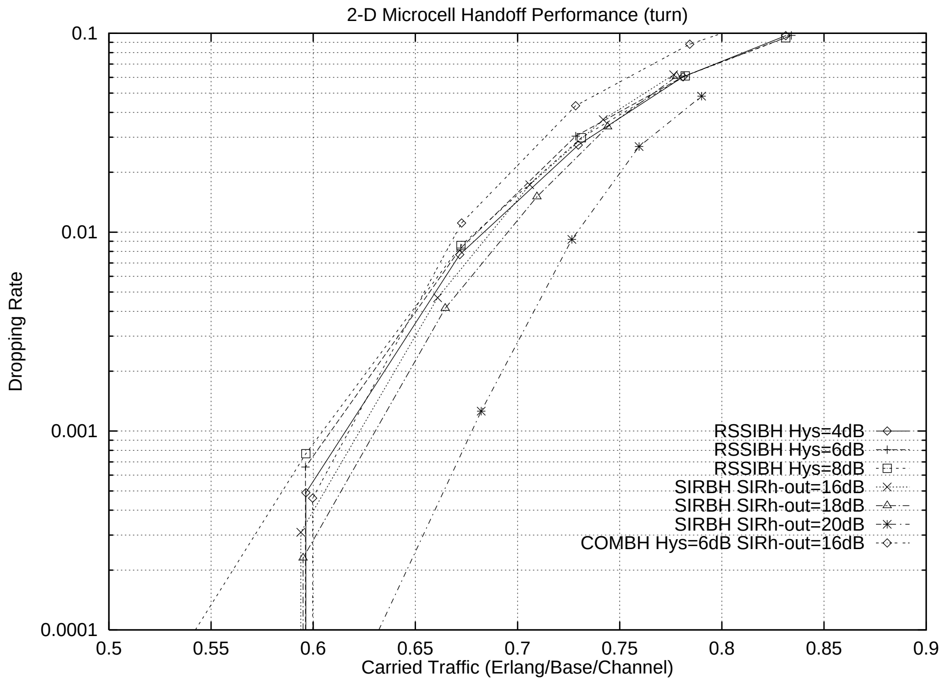

Figure 5.25: Dropping Rate of 2-D Microcell (turn)

one simulation, we set the probability of going straight through an intersection to 1, so that the MSs never turn left or right at any intersection. In the second simulation, we set the probability to 0, so that the MSs always turn left or right with equal probability in each direction. Figures 5.16, 5.18, 5.20, 5.22, 5.24 are the results of simulations with every MS going straight, and Figures 5.17, 5.19, 5.21, 5.23, 5.25 are the results of simulations with every MS always turning. The handoff distance in Figure 5.16 is the Line-Of-Sight distance from the point of handoff to the original BS. The handoff distance in Figure 5.17 is the sum of the distance from the point of the handoff to the corner and the distance from the corner to the original BS (which equals the 200 meters block size).

We find qualitatively similar results in both 2 dimensional simulations as we find in the 1 dimensional case. In addition, all the handoff schemes give higher average handoff distances and fewer handoffs in the "straight" case than they do in the "turn" case, because after turning around the corner, the path loss increases very rapidly, causing the MSs to handoff earlier.

It is interesting to note that, from Figures 5.18 and 5.19, the handoff numbers per call in the "turn" case are always greater than that in the "straight" case by roughly 1.5 for all the handoff schemes. This can be explained by the following analysis. First, consider a journey of a MS moving from a BS to a neighboring BS either in a "straight" case or a "turn" case. Before the MS reaches the cell boundary, i.e., the intersection, each handoff scheme works on the MS identically in both cases. In the "turn" case, after the MS has turned the corner, the MS has to handoff very quickly. Suppose the MS moving away from the original BS turned right at the corner. Because of the shadow fading, there is a probability of nearly 0.5 that the BS on the left side is the strongest BS and the MS is handed off to it. Whichever BS (the left or the right) the MS is handed off to, the rest of the journey towards the right BS will be the same as if the MS was moving originally from the left BS to the right BS in the "straight" case. Either case, the

MS will finally be handed to the right BS. But those MSs handed to the left BS at the corner will have to make one more handoff than those MSs handed to the right BS, and than those in the "straight" case. Thus, for each cell entered, an MS that always turns typically makes an additional 0.5 handoffs. Second, note that the average call duration is 120 seconds and the average mobile speed is 40 km/hour (11.11 meters/sec) and the radius of the microcell is 200 meters. Thus, on average, each MS travels through $11.11 * 120/400 = 3.3$ cells. We conclude that each "turning" MS should make a number of additional handoffs per call that is slightly less than $3.3 * 0.5$.

All the handoff schemes have similar average transmit powers, handoff failure rates and dropping rates in the two cases. We notice that the SIRBH with hand-out SIR threshold equal to the target SIR 20dB has the lowest average transmit power, handoff failure rate and dropping rate. This is consistent with the results of the minimum power handoff (MPH) scheme in [8]. The difference between these two schemes is that the MPH keeps looking for the BS/channel combination which will allow the MS to use minimum transmit power, but here the SIRBH with hand-out SIR threshold equal to the target SIR will not look for another BS/channel until the MS cannot achieve the target SIR. As mentioned in [8], the high average number of handoffs of the SIRBH with 20dB SIR threshold here could be reduced by a system timer. It would be interesting to compare these two schemes directly. The COMBH scheme still has a higher dropping rate than the corresponding RSSIBH and SIRBH schemes and the reason for this is yet unknown.

5.4 Effects of Various Factors on Power Control

As we know that in a system with stationary MSs, the ADCPC scheme converges [20]. But, the rate of convergence of the power control is influenced by

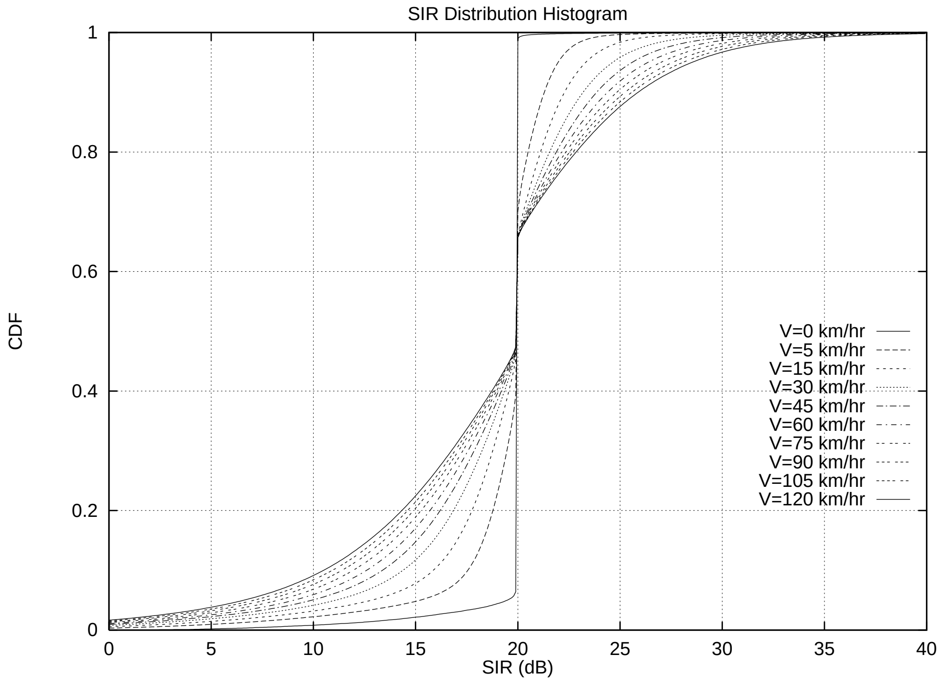

Figure 5.26: Empirical CDF of uplink SIRs in systems performing ADCPC with a target SIR of 20dB and varying MS speed.

many factors, including the rate of power control, the mobility of the MSs, the traffic load and the terrain characteristics, specifically the standard deviation of the shadow fading and the shadow fading correlation distance.

In order to find out the effect of power control rate and MS mobility on power control, we did simulations with different MS speed and power control rate in a 1-D macrocellular system. The system is performing LI-DCA, SIR threshold admission control and RSSIBH schemes. The system is also performing ADCPC with a target SIR, γ_t, of 20dB. In each simulation, all the MSs have the same speed, and the system has an offered traffic load of 0.5 Erlang/Base/Channel.

Figure 5.26 is an empirical CDF of the uplink SIR in a system with power control rate of once per second ($T_{pc} = 1$ second). For example, from Figure 5.26, we see that when all MSs travel at $V = 120$ km/hr, 0.4 represents the fraction of time that an arbitrary MS has an SIR of no more than 18 dB. We can see that when the MS speed is 0, the SIR is almost always close to the target SIR γ_t. But

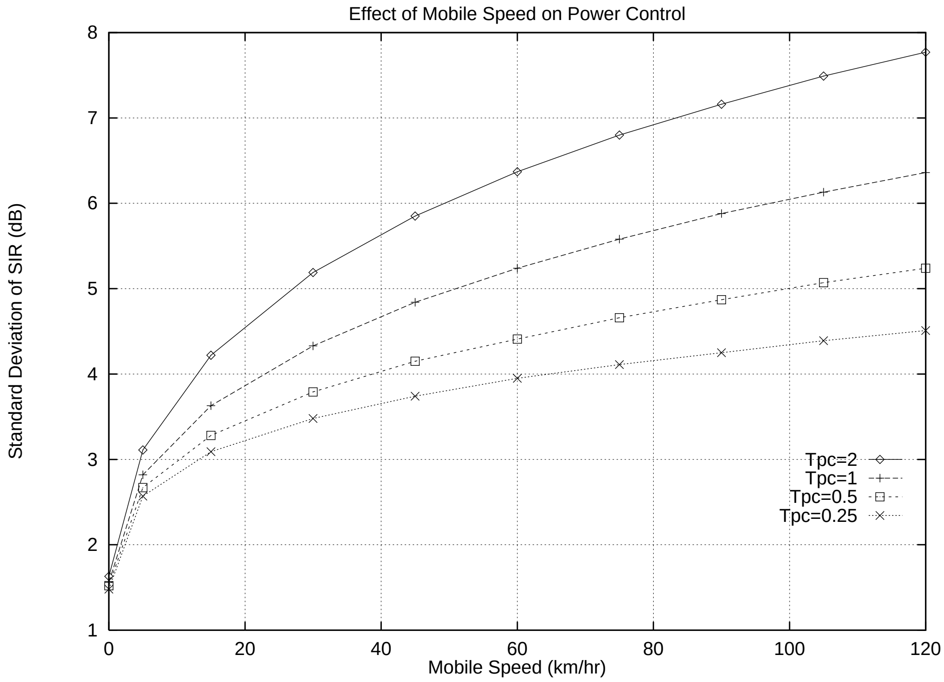

Figure 5.27: Standard deviation of uplink SIR in systems with different average MS speed and power control time. T_{pc} is the time between power control iterations.

as the MS speed increases, the SIR distribution becomes more dispersed around the target SIR γ_{t}.

Figure 5.27 shows the estimated standard deviation of the uplink SIR distribution histograms for different power control time intervals and varying average MS speed. Not surprisingly, we find that the faster the power control and the slower the average MS speed, the smaller the variation of SIR distribution and the more likely the SIR is close to γ_{t} in a power controlled system.

To identify the effect of traffic load on power control, Figure 5.28 plots the mean and standard deviation of uplink SIR from a simulation of a 1-D macrocellular system performing ADCPC with target SIR 20dB and LI-DCA with 23dB admission SIR threshold. The blocking and dropping rate plots of this simulation are already shown in Figures 5.1, 5.4 and 5.7. We find as the carried traffic load increases, the SIR distribution becomes more dispersed and the mean of SIR also

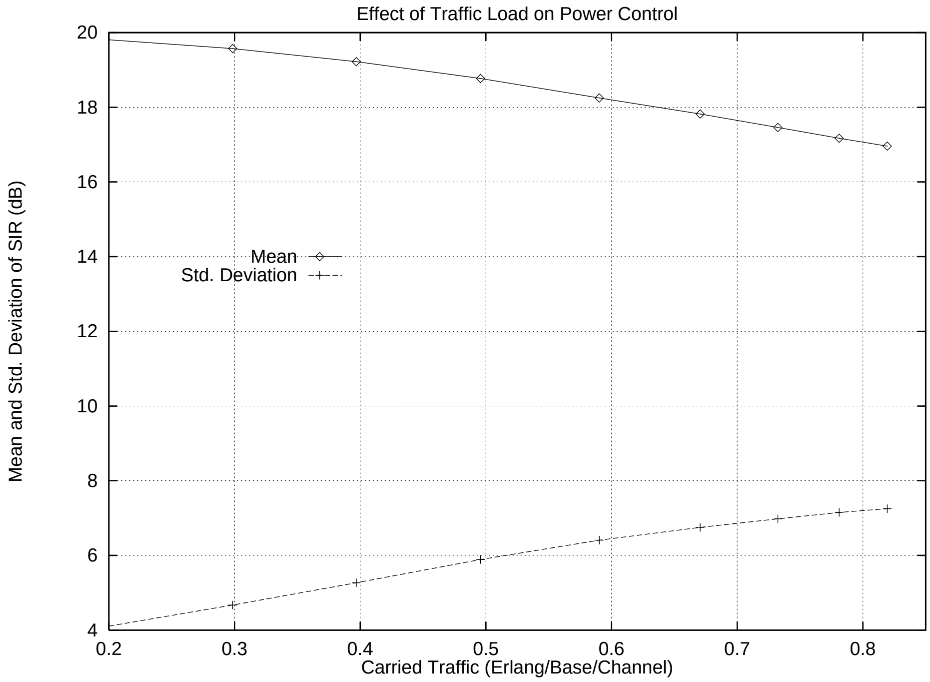

Figure 5.28: Mean and standard deviation of uplink SIR in systems with average MS speed 90km/hr and power control rate 1 time/second.

decreases from the target SIR. This implies that outages, which occur when the SIR of an MS is below the target SIR, become more likely with increasing offered load.

As for the effect of the terrain characteristics on power control, although we do not have any simulation results yet, we would reasonably expect that the higher the shadow fading and the shorter the shadow fading correlation distance, the more dispersed the SIR distribution and the higher the outage. In order to keep the outage of SIR, i.e., the QoS, under a acceptable level, it is therefore very important to set a margin between the target SIR every MS is trying to achieve, and the minimum SIR required by the QoS. The SIR margin should only be set after a careful study of the terrain characteristics where the system will be deployed, the average user speed, the power control rate and the average traffic load.

5.5 System Capacity of TDMA with IDRRM

It has been observed that an Integrated Dynamic Radio Resource Management of narrowband FDMA/TDMA system can greatly increase the system capacity in 1-D systems [18, 9, 8, 4]. We would like to see how it performs in 2-D macrocell and microcell cases.

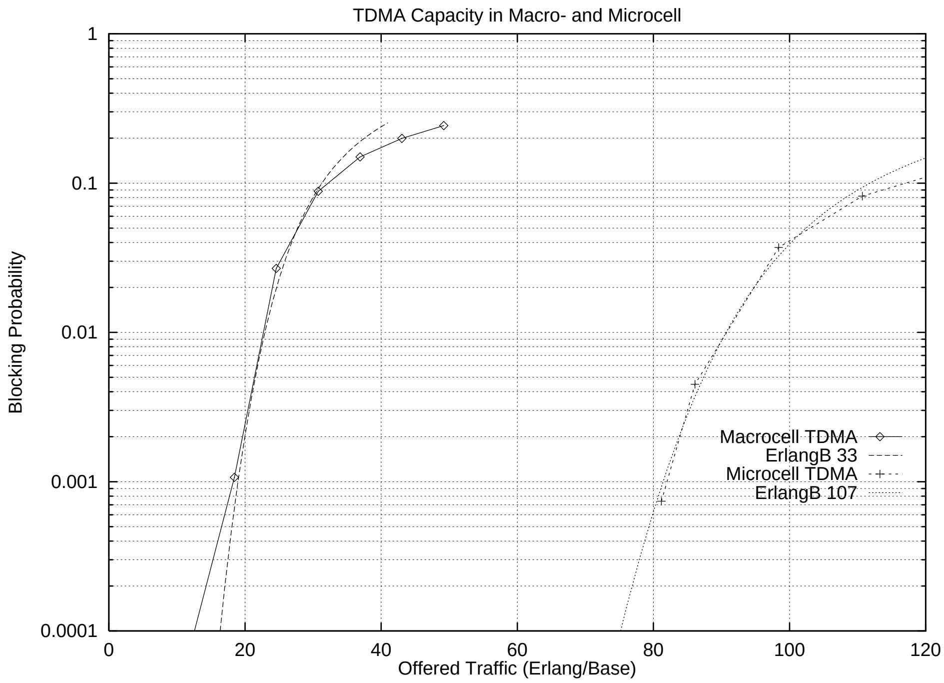

Figure 5.29: TDMA capacity in macrocells and microcells

We assume a system loosely based on the IS-54 FDMA/TDMA system with IDRRM for both 2 dimensional macrocell and microcell cases. For a 1.25MHz bandwidth, we have 123 TDMA communication channels. We assume the system would require an minimum SIR $\gamma_{\text{floor}} = 17$dB. If FCA were used, this would require a reuse factor of 7. Each cell will have $123/7 = 17.57$ channels. But with IDRRM, the system will achieve higher capacity. We assume the system performs ADCPC/LI-DCA/SIR admission threshold with power control rate of 1 adjustment/second. The SIR target is $\gamma_t = 20$dB and the SIR admission threshold is

$\gamma_{\text{new}} = 20$dB. We also assume the system performs RSSIBH with RSSI hysteresis of 9dB in macrocell case and 6dB in microcell case.

The simulation results are shown in Figure 5.29. The blocking rate plot of the macrocellular TDMA system is very close to the Erlang B blocking rate with 33 trunks. This is almost double of the 17.57 channels/cell of FCA. We can see that TDMA with integrated dynamic radio resource management can achieve almost twice the capacity as TDMA with FCA.

The high building between the streets provide very good isolation between cells, as we can see it from the microcellular TDMA plot, it is very close to the Erlang B blocking rate with 107 trunks. It seems that with integrated dynamic radio resource management in microcells, TDMA system can use most of the channels in every cell — close to the single cell system. We should mention that, in order to realize DCA and power control in TDMA systems, the time frame of all the BSs have to be synchronized.

Chapter 6
Conclusion

The principal result of this research has been to develop a simulation tool to study a wide range of issues in radio resource management. MADRAS V3 has the following capabilities:

- Exercise simultaneously a set of algorithms for power control, base assignment, channel allocation, admission control and handoff management.
- Simulate mobility of vehicles with random velocities.
- Simulate teletraffic conforming to an Erlang model.
- Simulate radio propagation, including attenuation and shadow fading in three physical environments: 1-D macrocell, 2-D macro- and microcell.

The simulator has been used to investigate several performance issues. The main results are:

- A new Active Channel Preservation DCA (ACP-DCA) and admission control scheme is proposed and investigated. From the simulation, the ACP-DCA scheme provide very little improvement over the simple LI-DCA with SIR admission threshold scheme. The future work will try to improve the proposed ACP-DCA scheme by allowing the arriving new MSs to participate one iteration of power adjustment, a scheme similar to the fast SAS scheme in [4] and investigate its performance together with other schemes.

- Three different handoff schemes, namely the RSSIBH, the SIRBH and the COMBH, are also studied. The RSSIBH scheme is shown to give the lowest dropping probability in 1-D macrocellular system. The SIRBH scheme with SIR hand-out threshold equal to the target SIR gives the lowest dropping probability and transmit power in the 2-D microcellular system. The COMBH scheme has lower average handoff distance and transmit power than the corresponding RSSIBH scheme with the same RSSI threshold and the SIRBH scheme with the same SIR threshold, but has higher dropping probability. The reason for this is still unknown and needs further investigation. The effect of handoff schemes on the MSs in the "straight" and "turn" cases is also studied.

- The effects of power control rate, mobile speed, the carried traffic load and the terrain characteristics on the power control are studied. The slower the power control rate and the higher the mobile speed, the more dispersed the SIR distribution and the more likely QoS outage becomes. Hence a larger SIR margin between the target SIR and the floor SIR required by the QoS is needed. Larger SIR margin is also needed as the traffic load becomes higher because of the same reason. Larger SIR margin is needed in urban areas than in rural areas. Future work will try to establish mathematical relationship between the SIR distribution and these factors.

- We find that TDMA systems with integrated dynamic radio resource management provides much greater capacity over TDMA systems with FCA. In addition, microcell systems can carry much higher load than macrocell systems. In the microcell case, each cell can use most of all the channels due to the good isolation between cells provided by the high buildings.

These results raise several issues that can be addressed in future studies. We would be interested to find whether there are any other Non-Interactive Admission control schemes which will perform better in protecting active calls and whether those IAC schemes will perform better with highly mobile MSs. We would further investigate the high dropping rate of COMBH scheme and also the relation between MPH and the SIRBH with SIR hand-out threshold equal to target SIR. Finally, the free flowing traffic mobility model may not be realistic. In particular, it would be desirable to investigate the performance of IDRRM under mobility models in which speeds are reduced on streets with heavy loads.

References

[1] CT2 Plus, A proposal for a Canadian common air interface standard. Issue 2.0. submitted to Radio Advisory Board Canada Industry Advisory Comm. Working Group Radio Interface Standards, Dec. 1990.

[2] D. Akerberg. Properties of a TDMA pico cellular office comunication system. In *IEEE GLOBECOM'88*, pages 1343–1349, Dec. 1988.

[3] M. Andersin, Z. Rosberg, and J. Zander. Soft admission in cellular PCS with constrained power control and noise. In *Proc. 5th WINLAB Workshop*, April 1995.

[4] M. Andersin, K. Sunell, and M. Frodigh. Distributed radio resource allocation in highway microcellular systems. In *Proc. 5th WINLAB Workshop*, April 1995.

[5] N. Bambos, S. Chen, and G. Pottie. Channel access algorithm with active link protection for wireless communication networks with power control. Technical Report UCLA-ENG-95-114, Dept. of Elec. Engi., UCLA, 1995. (submitted to IEEE/ACM Trans. Networking).

[6] N. Bambos and G. Pottie. On power control in high capacity cellular radio networks. In *Proc. 3rd WINLAB Workshop*, Oct. 1992.

[7] M. Cheng and J. Chuang. Distributed measurement-based dynamic channel assignment for wireless personal communications. In *Fifth Winlab Workshop on Third Generation Wireless Information Networks*, East Brunswick,NJ, April 1995.

[8] C.N. Chuah and R. Yates. Evaluation of a minimum power handoff algorithm. In *Sixth IEEE International Symposium on Personal, Indoor and Mobile Radio Communications PIMRC'95*, pages 623–627, 1995.

[9] C.N. Chuah, R. Yates, and D. Goodman. Integrated dynamic radio resource management. In *IEEE VTC-95*, pages 584–588, 1995.

[10] J. Chuang. Performance issues and algorithms for dynamic channel assignment. *IEEE J. Sel. Areas Commun.*, pages 955–963, Aug. 1993.

[11] W. Eriksson and R. Bownds. Performance of dynamic channel allocation in the DECT systems. In *Proc. IEEE VTC'91*, pages 693–698, May 1991.

[12] G. Foschini and Z. Miljanic. A simple distributed autonomous power control algorithm and its convergence. *IEEE Trans. Vehic. Tech.*, 42(4), November 1993.

[13] T. Fujii and M. Sakamoto. Reduction of cochannel interference in cellular systems by intra-zone channel reassignment and adaptive transmitter power control. In *Proc. IEEE VTC'88*, pages 668–672, 1988.

[14] P. Gaasvik, M. Cornefjord, and V. Svensson. Different methods of giving priority ot handoff traffic in a mobile telephone system with directed retry. In *Proc. 41st IEEE VTC*, pages 549–553, May 1991.

[15] D. J. Goodman, S. A. Grandhi, and R. Vijayan. Distributed dynamic channel assignment schemes. In *Proc. 43rd IEEE VTC*, 1991.

[16] S. Grandhi, R. Vijayan, and D. Goodman. A distributed algorithm for power control in cellular radio systems. In *Thirtieth Annual Allerton Conference on Communication, Control, and Computing*, Monticello, Illinois, Sep. 30-Oct. 2 1992.

[17] S. Grandhi, R. Vijayan, D. Goodman, and J. Zander. Centralized power control in cellular radio systems. *Accepted for publication in IEEE Trans. Vehic. Tech.*

[18] S. Grandhi, R. Vijayan, R. Yates, D. Goodman, and J. Holtzman. Distributed dynamic resource allocation. Technical Report WINLAB-TR58, WINLAB, Rutgers Univ., July 1993.

[19] S. Grandhi and J. Zander. Constrained power control in cellular radio systems. In *Proc. IEEE VTC'94*, pages 824–828, June 1994.

[20] S. Grandhi, J. Zander, and R. Yates. Constrained power control. *International Journal of Wireless Personal Communications*, 1(4), 1995.

[21] O. Grimlund, J-E. Berg, and B. Gudmundson. Handover performance in microcellular systems. In *MRC'91*, Nice, Nov 13-15 1991.

[22] B. Gudmundson and O. Grimlund. Handoff in microcellular based personal telephone systems. In *Proc. of WINLAB Workshop'90*, East Brunswick,NJ, Oct. 1990.

[23] M. Gudmundson. Analysis of handover algorithms in cellular radio systems. Technical Report TRITA-TTT-9107, Royal Institute of Technology, Sweden, 1991.

[24] M. Gudmundson. Correlation model for shadow fading in the mobile radio systems. *IEEE Electronics Letters*, 27(23):2145–2146, Nov. 1991.

[25] S. Hanly. An algorithm for combined cell-site selection and power control to maximize cellular spread spectrum capacity. *IEEE J. Sel. Areas Commun.*, 1995. (to appear).

[26] D. Hong and S. Rappaport. Traffic model and performance analysis for cellular mobile radio telephone systems with prioritized and nonprioritized handoff procedures. *IEEE Trans. Vehic. Tech.*, VT-35(3):77–92, Aug. 1986.

[27] I. Horikawa and M. Hirono. A multi-carrier switching TDMA-TDD microcell telecommunication system. In *Proc. IEEE VTC'90*, pages 167–171, May 1990.

[28] T. Kanai. Autonomous reuse partitioning in cellular systems. In *Proc. 42nd IEEE VTC*, pages 782–785, 1992.

[29] P. S. Kumar, R. Yates, and J. Holtzman. Power control based on Bit Error Rate (BER) measurements. In *Proc. IEEE Military Communications Conference MILCOM'95*, November 1995.

[30] W. Lee. *Mobile Communications Engineering.* McGraw-Hill, 1982.

[31] W. Mende. Evaluation of a proposed handover algorithm for the GSM cellular system. In *Proc. 40th IEEE VTC*, pages 264–269, May 1990.

[32] D. Mitra. An asynchronous distributed algorithm for power control in cellular radio systems. In *Proc. 4th WINLAB Workshop*, 1993. also in Wireless and Mobile Communications, pp. 177-186, Kluwer Academic Publishers, 1994.

[33] A. Motley. Advanced cordless telecommunication service. *IEEE J. Sel. Areas Commun.*, Vol. SAC-5:774–782, June 1987.

[34] T. Nagatsu, T. Tsuruhara, and M. Sakamoto. Transmitter power control for cellular land mobile radio. In *Proc. IEEE Globecom*, pages 1430–1434, 1983.

[35] R. Nettleton. Traffic statistics in a self-organizing cellular telephone system. In *Proc. IEEE VTC'90*, pages 305–310, May 1990.

[36] R. Nettleton and H. Alavi. Power control for spread-spectrum cellular mobile radio system. In *Proc. IEEE VTC'83*, pages 242–246, 1983.

[37] R. Nettleton and G. Schloemer. A high capacity assignment method for cellular mobile telephone systems. In *Proc. IEEE VTC'89*, pages 359–367, May 1989.

[38] H. Ochsner. Radio aspects of DECT. In *PROC. 4th Nordic Seminar Digital Mobile Radio Commun.*, June 1990. Paper 6.4.

[39] Uzi Timor. Dynamic resource allocation with active link protection. unpublished draft, August 94.

[40] W. Tschirks. Effects of transmission power control on the cochannel interference in cellular radio networks. *Electrotechink und Informationstechnik*, 106(5), 1989.

[41] R. Vijayan and J. Holtzman. Analysis of handoff algorithm using nonstationary signal strength measurements. In *Proc. Globecom'92*, Dec. 1992.

[42] R. Vijayan and J. Holtzman. A model for analyzing handoff algorithms. *IEEE Transactions on Vehicular Technology*, August 1993.

[43] H. Xie and S. Kuek. Priority handoff analysis. In *Proc. 43rd IEEE VTC*, May 1993.

[44] R. Yates. A framework for uplink power control in cellular radio systems. *IEEE J. Sel. Areas Commun.*, 13(7):1341–1348, September 1995.

[45] R. Yates and C. Y. Huang. Constrained power control and base station assignment in cellular radio systems. *IEEE/ACM Transactions on Networking*, Sept. 1995. to appear.

[46] R. Yates and C. Y. Huang. Integrated power control and base station assignment. *IEEE Trans. Vehic. Tech.*, 44(3), August 1995.

[47] J. Zander. Distributed cochannel interference control in cellular radio systems. *IEEE Trans. Vehic. Tech.*, 41(3), August 1992.

[48] J. Zander. Performance of optimum transmitter power in cellular radio systems. *IEEE Trans. Vehic. Tech.*, 1992.

[49] J. Zander. Transmitter power control for cochannel interference management in cellular radio systems. In *Proc. 4th WINLAB Workshop*, Oct 1993.

[50] N. Zhang and J. Holtzman. Analysis of handoff algorithms using both absolute and relative measurements. In *Proc. IEEE VTC'94*, pages 82–86, 1994.